Shear buckling coefficients for longitudinally stiffened haunched steel plate girders

Mariana Echeverri Loaiza

Universidad Nacional de Colombia

Facultad de Minas, Departamento de Ingeniería Civil

Medellín, Colombia

2024

Shear buckling coefficients for longitudinally stiffened haunched steel plate girders

Mariana Echeverri Loaiza

Thesis presented as a requirement to qualify for the title of:

Civil engineer

Advisor:

Ph.D., Carlos Alberto Graciano Gallego

Research line:

Structural Stability - Numerical Analysis

Grupo de Investigación:

Mecánica Computacional y Análisis de Estructuras

Universidad Nacional de Colombia

Facultad de Minas, Departamento de Ingeniería Civil

Medellín, Colombia

2024

To my parents, Carlos and Nancy,

who have given me everything in life.

Acknowledgements

Resumen

En esta tesis se investiga en profundidad el comportamiento crítico a pandeo de vigas de placa de acero acarteladas sometidas a cargas de corte. El estudio se realiza mediante análisis de pandeo lineal utilizando el método de elementos finitos. Primero, los resultados se validan con resultados anteriores para paneles de alma no rectangulares simplemente apoyados. A continuación, se lleva a cabo un extenso estudio paramétrico para investigar la influencia de varios parámetros geométricos, incluido el ángulo de inclinación, la relación de aspecto del panel, el tamaño de las aletas y la presencia de rigidizadores longitudinales en los coeficientes de pandeo. Finalmente, los resultados se emplean para desarrollar expresiones para los coeficientes de pandeo por cortante para vigas de placa de acero rigidizadas longitudinalmente teniendo en cuenta los parámetros mencionados anteriormente.

Palabras clave: vigas esbeltas, rigidización longitudinal, pandeo elástico, modelado numérico, carga crítica.

Abstract

In this thesis, the critical buckling behavior of haunched steel plate girders subjected to shear loading is investigated in depth. The study is conducted through linear buckling analysis using the finite element method. First, the results are validated with previous results for simply supported nonrectangular web panels. Thereafter, an extensive parametric study is conducted to investigate the influence of various geometric parameters including the inclination angle, the panel aspect ratio, the size of the flanges and the presence of longitudinal stiffeners on the buckling coefficients. Finally, the results are employed to develop expressions for the shear buckling coefficients for longitudinally stiffened-haunched steel plate girders taking into account the aforementioned parameters.

Keywords: Plate girders, longitudinal stiffening, elastic buckling, numerical modeling, critical load.

Content

List of figures

List of tables

Notation and symbols

Roman Letters

a	Length of web panel
b_f	Width of flange
b_{st}	Width of stiffener
D	Flexural rigidity of unit width of the web plate
E	Young's modulus
h_0	Shorter side
h_1	Longest side
h_{st0}	Stiffener position on the shorter side
h_{st1}	Stiffener position on the longest side
I_{st}	Effective second moment of area of stiffener
k_f	Buckling coefficient
k_s	Buckling coefficient for shear buckling
t_f	Flange thickness
t_{st}	Stiffener thickness
t_w	Web thickness

Greek Letters

γ_s	Relative flexural rigidity of the longitudinal stiffener
υ	Poisson's ratio
ϕ	Angle that the inclined flange forms with the horizontal

Abbreviations

FE	Finite element

Glossary

buckling coefficient: a dimensionless parameter that depends on the boundary and loading conditions, and the geometric dimensions of the plate girder.

critical load: also known as buckling load, is the maximum load which a straight elastic plate member can assume a deflected position.

global buckling: overall buckling mode of the web plate, in which the web plate buckles together with the stiffener.

local buckling: also known as web crippling, failure mode of the directly loaded panel in which the stiffener forms a nodal line and effectively controls the out-of-plane deflection of the web plate.

longitudinal stiffener: longitudinal reinforcement employed to increase the resistance of plate girders subjected to transverse loads and used to prevent buckling of the plate girder.

plate girder: a welded I-beam fabricated from separate structural steel plates.

1. Introduction.

In the field of steel bridge construction, the selection and design of structural components are important to ensure both the structural integrity and economic feasibility of the project. A critical decision in this process is the choice between laminated and plate girders, a selection that significantly influences the overall design and cost-effectiveness of the bridge.

Traditional hot-rolled I-beam sections (also known as laminated sections), while common, often fall short in scenarios involving excessive loads or expansive spans due to their insufficient capacity, leading to designs that are not economically viable. In contrast, plate girders, crafted through the meticulous welding of separate steel plates to form an I-shaped beam, present a superior alternative. The reason why this happens is because, in laminated profiles, the increase in resistance capacity is achieved only by increasing the section area. This means a greater amount of material and therefore an increase in cost. On the contrary, with plate girders, by increasing the slenderness of the web we achieve an increase in the resistant capacity, keeping the section area constant, without wasting material. Furthermore, with more stylized sections the aim is also to reduce the weight of the structure as much as possible so that a good part of the load capacity is available for traffic loads and not absorbed by the weight of the structure itself.

a) laminated section   b) plate girder
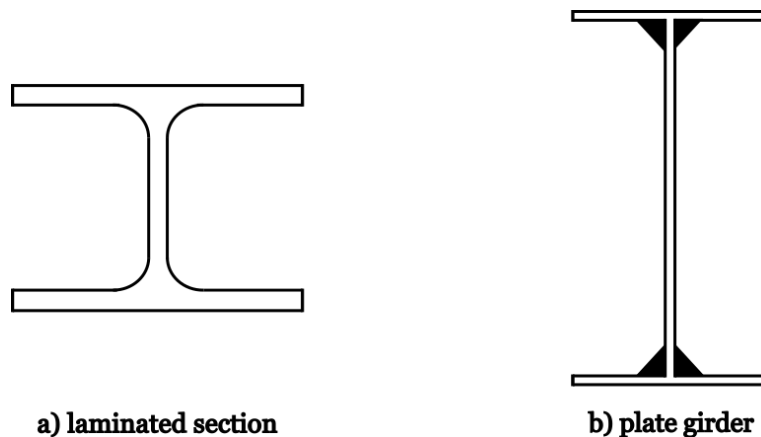
Figure 1-1. Laminated and plate girder.

In addition to their high load-carrying capacity, plate girders' custom fabrication process provides flexibility to create non-prismatic shapes (i.e., tapered web depth) consistent with the demand variation along the girder spans. This flexibility results in significant material savings compared to otherwise prismatic sections (i.e., identical cross-sections along the entire span), which in turn produce more economical designs [1].

The advantages of opting for tapered or non-prismatic designs extend beyond material efficiency. Such girders, with their gradually changing inertia, facilitate a more effective distribution of stress within the web panel, further contributing to reductions in steel usage and the overall cost of the structure. Moreover, the trapezoidal shape of these panels proves advantageous in structures requiring non-standard shapes or incorporating pre-formed service openings, thereby enhancing the aesthetic appeal and functional utility of the bridge.

However, the design of tapered plate girders introduces its own set of challenges, primarily concerning the global instability caused by the high slenderness of the web panels. To address this, the incorporation of transversal and longitudinal stiffeners becomes imperative. These stiffeners play a critical role in limiting slenderness and preventing excessive deformation of the web, thereby maintaining the structural integrity of the girder. The design process thus involves a careful optimization between the material and manufacturing costs against the expected improvement in strength (obviously, the use of additional stiffening increases the overall cost of fabrication). This often leads to the adoption of equally spaced transverse stiffeners as a common solution, which, by providing the necessary rigidity, creates nodal lines that restrict the buckling of the web to the panels between stiffeners. In cases where it is necessary to reduce the distance between stiffeners, the use of longitudinal stiffeners may offer a more economical solution.

Figure 1-2. Girder web depth transition on Mississippi River Bridge [2].

The design considerations for plate girders predominantly focus on managing shear forces, especially given that, in most practical ranges of span lengths, the induced shearing force tends to be relatively low compared to the axial forces in the flanges resulting from flexure. As a result, the thickness of the web plate is generally much smaller than that of the flanges. Consequently, the web panel buckles at a relatively low value of the applied shear loading.

Despite the advantages mentioned in this introduction about longitudinally stiffened haunched steel plate girders, very few research and construction codes clearly define equations and procedures for their design and construction. In other investigations, equations for critical and ultimate load of rectangular (and non-rectangular) girders without stiffening have been studied. However, there are very few articles focused on longitudinal stiffening. Some of those found only define the optimal position of the stiffener but do not define design equations as such.

As seen above, there is still a need to investigate the critical buckling response of longitudinally stiffened-haunched girders subject to shear. Therefore, this thesis aims at investigating the linear buckling response of this type of girders. The study is conducted numerically through linear buckling analysis using the finite element method. Firstly, a numerical model is built for simply supported rectangular panel subject to shear loading. Once the model is validated, the geometry is extended to longitudinally stiffened-haunched girders. After that, a parametric analysis is performed to investigate the influence of various geometric variables including the inclination angle, the panel aspect ratio, the size of the flanges and the presence of longitudinal stiffeners on the buckling coefficients. In the end, the results from the parametric study are employed to develop expressions for the shear buckling coefficients for longitudinally stiffened-haunched steel plate girders.

1.1. Four typologies – general behavior.

It is important to clarify that four types of panels classified by Bedynek [3] are evident in the literature, but not all of them are relevant in this thesis; the reasons will be explained below.

Some numerical studies presented in the past demonstrated that both the critical load and ultimate strength of a tapered plate girder are strongly influenced by two factors: (1) the inclination of the flange and whether the flange is under tension or compression and (2) the direction of the developed stress field. , which can appear on the diagonal of the short

or long network. As a result, it is possible to distinguish four different typologies of conical plate beams (see Figure 1-3):

I. inclined flange in compression and diagonal tension field developed in the short diagonal.

II. inclined flange in tension and diagonal tension field developed in the long diagonal.

III. inclined flange in tension and diagonal tension field developed in the short diagonal.

IV. inclined flange in compression and diagonal tension field developed in the long diagonal.
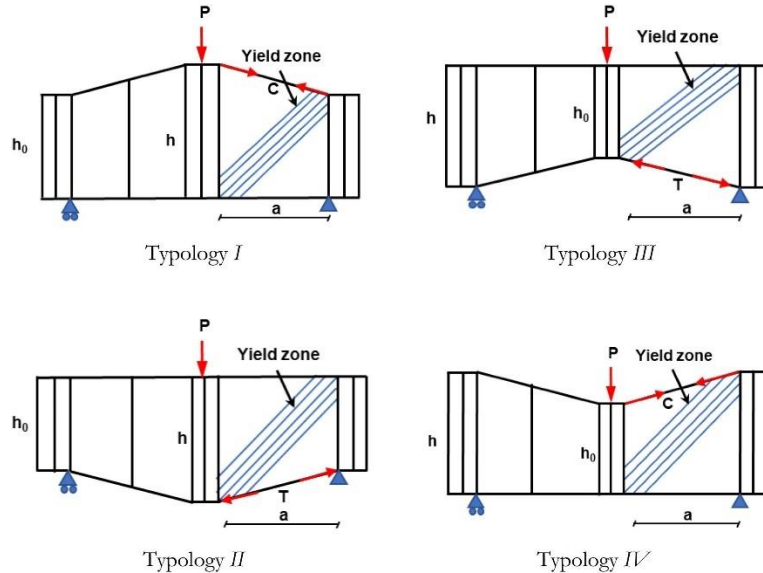
Figure 1-3. Four typologies of tapered plate girders [4].

Figure 1-4 shows examples of the application of each typology. Three of them can be met in various parts of a bridge span with a non-prismatic cross-section, depending on the distribution of internal forces. The most common case is the first one, which appears frequently near to the intermediate supports of continuous bridges or in portal frames. That is why this thesis just includes this last type of configuration: where the tension field is developed in the short diagonal and the inclined flange is under compression, due to its importance in practical engineering use.
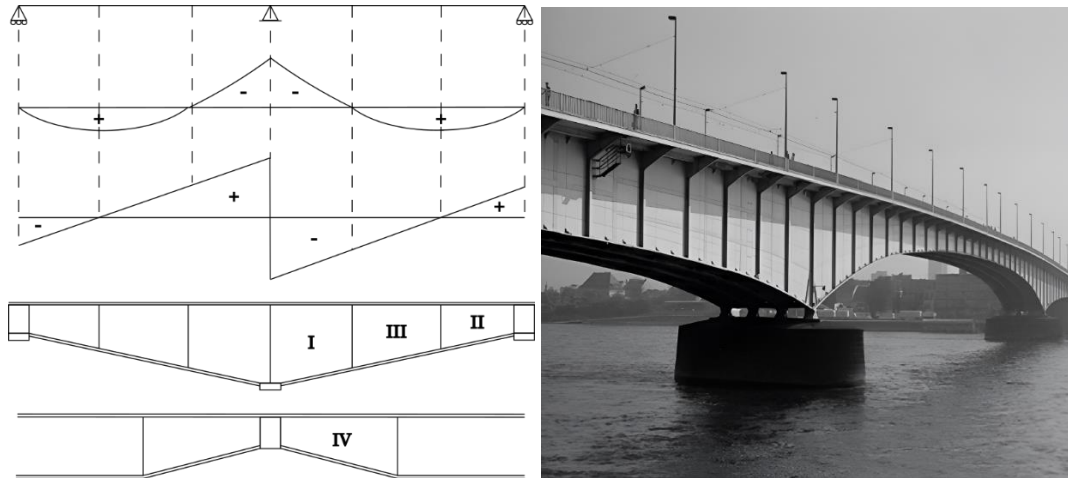
Figure 1-4. Tapered plates in continuous steel bridges [3].

1.2. Aims and objectives.

The main objective of this thesis is the development of a reliable design tool to assess the shear buckling coefficients of longitudinally stiffened steel plate girders. To achieve this goal some intermediate tasks had to be done:

- Review the literature to investigate what has been studied regarding the buckling coefficient in stiffened and unstiffened girders, both rectangular and haunched.

- Review the numerical models available in the literature for calculating the critical shear load of these girders.

- Study numerical models used to consider the effect of longitudinal stiffening on the critical load of slender haunched steel girders subjected to shear.

- Preparation of the numerical model using finite elements.

- Validation of the model using numerical results from the literature.

- Study the effect of longitudinal stiffening systems on the critical shear resistance: straight stiffeners, inclined stiffeners, among others.

 - Develop expressions for shear buckling coefficients taking into account a large set of parameters.

1.3. Method.

The method to find the equation that defines the buckling coefficients in longitudinally stiffened girders consists of developing numerical models using finite element software, in

this case, Ansys 2024 R1, which allows studying the effect of longitudinal stiffening on the critical load of said haunched steel plate girders subjected to shear. This is done through a parameterization of different variables in order to find the influence of each on the buckling coefficients, and thus be able to develop a reliable and generalizable equation.

1.4. Limitations.

This thesis investigates the buckling coefficients in longitudinally stiffened tapered plate girders under critical load conditions. The primary focus is on shear load, as there is a lack of research on the ultimate load capacity for these structures. Understanding the critical load is a prerequisite for determining the ultimate load capacity, thus this study serves as a foundational step toward comprehensive load capacity analysis. Limitations of this study include:

1. The analysis is confined to the critical load condition. The ultimate load capacity, which provides insights into the maximum load the structure can withstand before failure, is not covered. Future research is needed to bridge this gap and extend the findings to ultimate load scenarios.
2. The investigation is limited to shear load. The combined effect of shear and bending moments, which is a common scenario in real-world applications, is not addressed in this study. Subsequent research could explore these combined load conditions to provide a more holistic understanding of the structural behavior.
3. The research focuses exclusively on longitudinally stiffened tapered plate girders. Other forms of stiffening and different girder geometries are not considered, potentially limiting the applicability of the findings to a broader range of structural designs.
4. Empirical validation of the theoretical models is beyond the scope of this thesis. Future studies incorporating experimental or field data could enhance the reliability of the proposed models.
5. The influence of material properties, such as steel grade variability and its impact on buckling behavior, is not thoroughly examined. Future investigations could include a detailed analysis of material property variations to assess their effect on the critical load capacity.

These limitations delineate the scope of the current study and highlight areas for future research to expand our understanding of the behavior of longitudinally stiffened tapered plate girders under various load conditions.

1.5. Outline of contents.

Chapter 1 contains the introduction to the problem to be studied and its justification, in addition to the objectives and limitations of the study presented.

In Chapter 2 there is a review of the literature on rectangular and prismatic girders, both stiffened and unstiffened. The equations for buckling coefficients that have been developed for some specific cases are presented.

Chapter 3 presents the analysis through a finite element program. The geometry and material used, loading and boundary conditions, mesh convergence analysis and model validation are presented.

Chapter 4 presents the parametric study carried out and the variables that were varied with their respective justification.

Chapter 5 presents the first discussions of the results obtained through the parametric study. The influence of the flexural rigidity of the stiffeners, the slenderness of the web, the aspect ratio, the thickness ratio and the inclination of the haunch are found, and the forms of buckling originate are discussed.

In Chapter 6, the equation for the buckling coefficient is proposed, explaining the procedure for obtaining it and the statistical evaluation of itself. It is also compared with design code equations.

2. Models for plate girders.

To begin to address the problem, it is necessary to carry out a study of the research that has been carried out in the past, in order to have a solid base of knowledge and begin to understand the problem from its beginnings. Additionally, learn from the procedures that have been used previously to obtain buckling equations for other specific cases.

This is why in this section a summary will be made of the most relevant articles, theses and codes found, which managed to obtain an equation for the buckling coefficients for each of the specific cases written there. The boundary conditions, geometry, loading conditions, among other characteristics, that led each of these authors to find these equations are summarized. Between Sections 2.1 to 2.9, the rectangular and prismatic plates that are not stiffened are detailed. Then, between Sections 2.8 to 2.10, the rectangular and prismatic plates that are longitudinally stiffened are explained.

2.1. Timoshenko and Gere [5].

The foundational framework for predicting the elastic shear buckling strength of prismatic web panels was introduced by Timoshenko and Gere [5], drawing from an analytical perspective on the elastic buckling behavior of plates under shear stress. In this seminal work, the web panel is treated as if it were simply supported on all sides, with the influence of the flange on the web's stability overlooked. Key factors determining this model include the web's slenderness ratio (b/t), the modulus of elasticity (E), Poisson's ratio (v), and a buckling coefficient (k) that depends on the aspect ratio of the web panel ($\alpha = a/b$), as delineated in Eqs. (1)- (2).

$$\tau_c = k * \frac{\pi^2 * E}{12 * (1 - v^2) * (b/t)^2} \tag{1}$$

$$k = \frac{9 * \pi^2 (1 + \alpha^2)^2}{32 * \alpha^3} \tag{2}$$

In the period following Timoshenko's initial proposal regarding the coefficient, extensive research was conducted by various authors aiming to refine the calculation of critical stresses, focusing on achieving more accurate estimates of the parameter k. The milestone of achieving an exact solution was first reached by Southwell and Skan in 1924 [6], who determined a value of $k = 5.34$ for panels of infinite length ($\alpha = \infty$). Subsequently, in 1933, Seydel [7] discovered the exact solution for $k = 9.34$ when $\alpha = 1$. Efforts by Bergmann and Reissener in 1932 also aimed to refine these values. However, it was Stein and Neff's [8]

24

publications in 1947 that presented the most precise solutions for various aspect ratios α, leading to the development of the parabolic equations (Eqs. (3)-(4)) still in use today for approximating these findings with considerable accuracy.

$$k = 4 + \frac{5.34}{(a/b)^2} \text{ for } (a/b) < 1 \tag{3}$$

$$k = 5.34 + \frac{4}{(a/b)^2} \quad \text{for } (a/b) > 1 \tag{4}$$
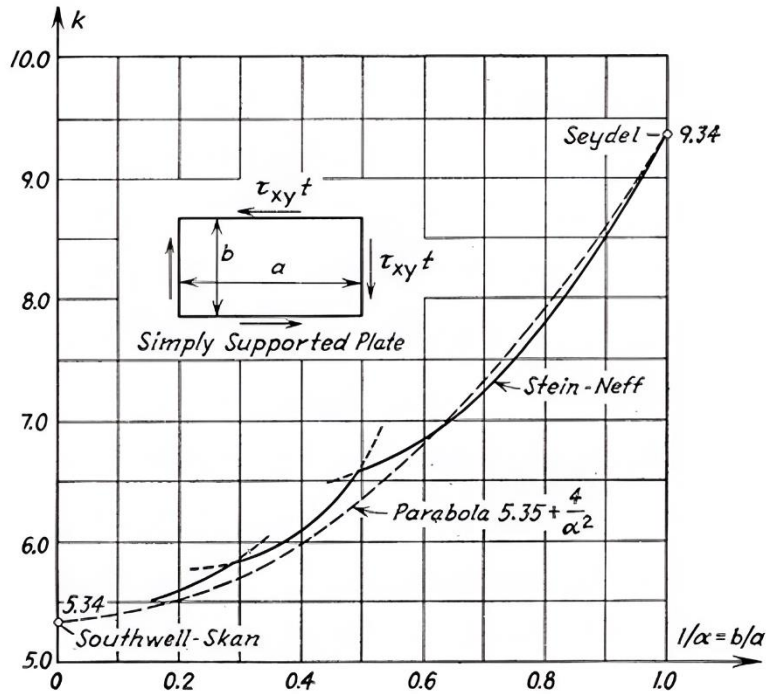
Figure 2-1. Panels simply supported on all four edges [9].

2.2. Lee [10].

Lee [10] conducted a numerical analysis of how various geometric parameters influence buckling coefficients in web panels, utilizing finite element methods. This study involved simulating a segment of a plate girder positioned between two transverse stiffeners, aiming to derive straightforward design formulas for two specific scenarios: one where the junction between the flange and web is simply supported, and another where it is clamped, as detailed in Eqs. (5)- (8).

$$k_{ss} = 4 + \frac{5.34}{(a/D)^2} \quad \text{for } (a/D) < 1 \tag{5}$$

$$k_{ss} = 5.34 + \frac{4}{(a/D)^2} \quad \text{for } (a/D) > 1 \tag{6}$$

$$k_{sf} = \frac{5.34}{(a/D)^2} + \frac{5.34}{(a/D)} - 3.44 + 8.39 * (a/D) \text{ for } (a/D) < 1 \tag{7}$$

$$k_{sf} = -\frac{1.99}{(a/D)^3} + \frac{5.61}{(a/D)^2} + 8.98 \ \text{for} \ (a/D) \geq 1 \tag{8}$$

2.3. Mirambell and Zárate [11].

These models enhance Timoshenko and Gere's framework by incorporating additional coefficients to capture the effects of tapering. Specifically, Mirambell and Zárate [11] introduced a model, grounded in numerical analysis, to calculate the shear buckling coefficient ($k_{M\&Z}$). This model takes into account several factors: the web aspect ratio ($\alpha = a/h_1$), the angle of flange inclination ($\tan(\phi)$), the ratio of flange width to thickness ($\lambda_f = b_f/t_f$), and the ratio of flange width to web depth ($\eta = b_f/h_1$), as outlined in Eqs. (9) - (10). It's important to note, however, that their approach is tailored to a specific geometric configuration, where the diagonal tension field—emerging during the post-buckling phase—is oriented in the shorter direction, with the inclined flange subjected to tension.

$$k_{M\&Z} = \left(c_1 * \eta^{c_2} - c_3 * \eta^{-c_4} * \lambda_f - 4\right) + \frac{4}{\alpha^2} - 5 * tg\phi^{0.8} * (\alpha - 1) \ \text{for} \ \alpha \geq 1 \tag{9}$$

$$k_{M\&Z} = \left(c_1 * \eta^{c_2} - c_3 * \eta^{-c_4} * \lambda_f - 5.34\right) + \frac{5.34}{\alpha^{1.8}} + 2 * tg\phi^{0.8} * (\alpha - 1) \ \text{for} \ \alpha < 1 \tag{10}$$

2.4. Bedynek et al. [12].

Bedynek et al. [12] conducted a numerical analysis aimed at estimating the shear buckling strength of tapered web panels. In their approach, they modeled the tapered web panel as a trapezoidal plate with simple supports, intentionally omitting the influence of flanges. They formulated predictive equations (referenced as Eqs. (11)-(14) which were derived by considering variations in aspect ratio, taper angle, web thickness, and different geometric configurations. These configurations are described as follows: (i) Typologies 1 and 3, which depict tapered plate girders with a tension field oriented in the shorter direction, where the inclined flange is subject to compression and tension, respectively; and (ii) Typologies 2 and 4, which illustrate tapered plate girders with a tension field oriented in the longer direction, where the inclined flange is subject to tension and compression, respectively.

$$k_{B1} = 5.5 * \alpha^{0.8} * \tan(\phi) + 8.7 * \alpha^{-0.4} \tag{11}$$

$$k_{B2} = 10.6 * \alpha^{0.5} * \tan(\phi) + 8.0 * \alpha^{-0.4} \tag{12}$$

$$k_{B3} = 47 * \alpha^{1.8} * tan^2(\phi) + (-0.5 * \alpha^2 + 3.7 * \alpha + 0.3) * \tan(\phi) + (0.5 * \alpha^2 - 4.2 * \alpha + 13) \tag{13}$$

$$k_{B4} = 62 * \alpha^{1.6} * tan^2(\phi) + (-0.7 * \alpha^2 + 4.6 * \alpha - 2.8) * \tan(\phi) + (0.44 * \alpha^2 - 3.4 * \alpha + 12) \qquad (14)$$

2.5. Serror et al. [13].

Serror et al. [13] undertook a regression analysis based on finite element (FE) outcomes, leading to the proposition of new design guidelines for both elastic and nominal shear strength. The primary aim of this analytical effort was to scrutinize the impact that varying geometric dimensions of tapered-end web panels have on elastic shear buckling and nominal shear strength. Their analysis encompassed four distinct panel typologies: those with short diagonal tension with and without stiffeners, and those with long diagonal tension with and without stiffeners. This investigation resulted in the derivation of two equations where $K = K_1 * K_2 * K_3$. However, the complexity of these formulas is highlighted by the inclusion of over 62 variable parameters, encompassing both functions (f_i) and constants (c_i), which renders the equations challenging to apply broadly and limits their practical utility.

2.6. Ibrahim et al. [14].

Ibrahim et al. [14] carried out an extensive finite element analysis study to estimate the critical buckling coefficients for tapered steel webs. Three boundary conditions for the web plate were included: simply supported edges, flange restrained edges and fixed edges. The studied parameters are: the tapering ratio of the panel, the panel's normalized length and the flange-to-web thickness ratio. Three loading conditions were considered: uniform compression, pure bending and pure shear. They developed formulas for tapered web plates coefficients of buckling for the load conditions mentioned above. For pure shear are

$$k_{ss} = 5.907 - \frac{0.604}{R^2} + \frac{8.202}{\alpha} - \frac{6.748}{\alpha R} \qquad (15)$$

$$k_{ff} = 9.775 - \frac{0.558}{R^2} + \frac{13.558}{\alpha} - \frac{12.358}{\alpha R} \qquad (16)$$

$$k_{FR} = k_{ss} + \beta(k_{ff} - k_{ss}) \qquad (17)$$

$$\beta = (t_f/t_{fw}) - 0.64 - 0.16 * (t_f/t_{fw})^2 \leq 1 \qquad (18)$$

2.7. EC3: 1-5 [15].

Attributed to the unavailability of standardized design expressions for calculating the shear buckling strength of tapered plate girders, the EC3: 1-5 1993 [15] recommends the model proposed by Timoshenko and Gere for prismatic plate girder (see Eqs. (3)-(4)) to be used

for estimating the shear buckling strength of the tapered web panel with some modifications.

These modifications included using the smaller panel depth for calculations when the taper angle is less than 10° and using the larger panel depth for larger taper angles.

2.8. Cook and Rocky [16].

Cook and Rocky [16] studied the critical shear buckling of infinitely long plates for both the simple support and clamped boundary conditions using transverse stiffeners made by closed section instead of open section stiffeners. Then, they continued their earlier work and were able to obtain a useful design relationship between the critical shear buckling stress and the ratio of the torsional to flexural rigidity of the stiffener as shown in Figure 2-2.
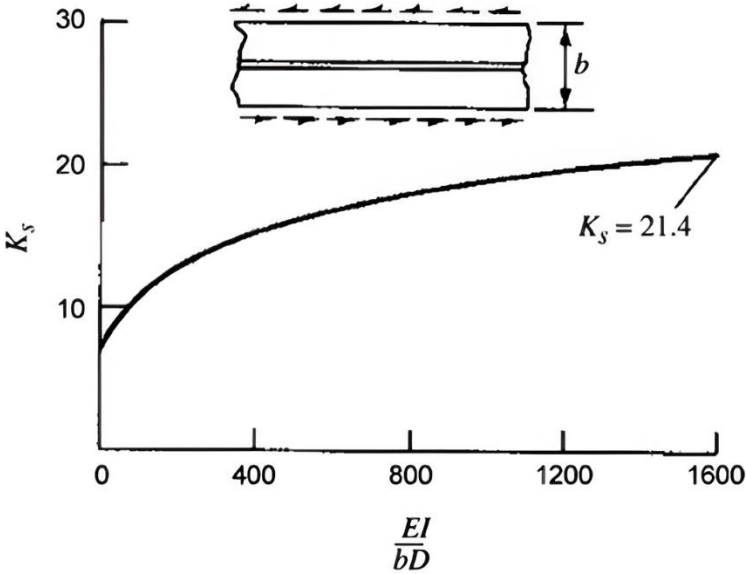
Figure 2-2. Variation of buckling coefficient for plates longitudinally stiffened under shear [16].

2.9. Höglund [17].

Höglund [17] presented the rotated stress field method and its comparison with results of Steel and Aluminum Plate Girders. He also proposed a design formula for girders with stiffeners at supports only, transversal, and longitudinal web stiffeners. The buckling coefficient k_H is given as a function of the stiffness parameter $\gamma_{st} = EI/h_w D$ for *one centric longitudinal stiffener in a long web panel.* The theoretical curve can be approximated by

$$k_H = 5.34 + 1.36 * \sqrt[3]{\gamma_{st}} \tag{19}$$

This value of k_H cannot directly be used in design because the post-buckling strength is much less in a stiffened web than in an unstiffened one. Therefore, the stiffness I of the stiffener is reduced with a factor of $I/3$. Inserting the reduced value $I = I_{st}/3$ and $D = Et_w/(12(1 - v^2))$ into (19) and using $v = 0.3$ gives

$$k_H = 5.34 + 2.1 * \sqrt[3]{I/h_w t_w^2} \tag{20}$$

2.10. EC3: 1-5 [15].

The EC3: 1-5 1993 [15] establishes, in addition to what is presented in Section 2.7, some equations to determine the buckling coefficient according to the aspect ratio and the position of the stiffeners used. If the aspect ratio $\alpha = a/h_w$ satisfies $\alpha \geq 3$ and it is a plate with one or two longitudinal stiffeners, it is applicable Eq. :

$$k_\tau = 5.34 + 4.00 * (h_w/a)^2 + k_{\tau sl} \tag{21}$$

$$k_{\tau sl} = 9 * (h_w/a)^2 \sqrt[4]{(I_{sl}/t^3 * h_w)^3} \text{ but not less than } \frac{2.1}{t} \sqrt[3]{I_{sl}/h_w} \tag{22}$$

For plates with one or two longitudinal stiffeners and the aspect ratio $\alpha = a/h_w$ satisfies $\alpha < 3$ it is applicable Eq. (23):

$$k_\tau = 4.1 + \frac{6.3 + 0.18(I_{sl}/t^3 * h_w)}{\alpha^2} + 2.2\sqrt[3]{I_{sl}/t^3 * h_w} \tag{23}$$

In addition to what was summarized here, other relevant research was found for longitudinally stiffened girders, among them are:

- Estrada et al. [18] found equations for the buckling coefficients for the specific case of stainless steel.
- Ferreira [19] proposed new practical insights about the ideal rigidity and position of the stiffeners, including the assessment of the optimum positions of longitudinally multi-stiffened plates under different normal stress ratios.
- Alinia [20] proposed an equation for critical shear stress for plates that have a single transverse stiffener.

3. Linear eigenvalue-buckling analysis.

In this chapter, finite element analysis of longitudinally stiffened haunched steel plate girders under shear loading is developed and checked. The models are developed using the software ANSYS 2024 R1 [21].

Shell 181 elements, with four nodes and six degrees of freedom (translations in the x, y, and z directions, and rotations about the x, y, and z-axes) on each node are employed to model the girder components (flanges, web and stiffener). This type of element is suitable for analyzing thin to moderately thick shell structures and is well-suited for linear, large rotation, and/or large strain nonlinear applications, so our case study is well covered with this type of modeling.

All the models are analyzed by running a linear eigenvalue-buckling analysis (because the objective of the analysis is to calculate the load at which the structure is expected to buckle). The software solves the governing equation:

$$[K + \lambda_i[S]]\{\psi_i\} = \{0\} \tag{24}$$

and the outcome of this analysis is the load multiplier (λ_i) and the mode shape (ψ_i). With the load multiplier and the applied load (in this case unit load), it is possible to obtain the critical buckling stresses τ_{cr}, and with this, solve the value of the shear buckling coefficient k_s. The critical buckling shear stress for a simply supported rectangular plate is expressed as

$$\tau_{cr} = k_s \frac{\pi^2 E}{12(1 - v^2)}(\frac{t_w}{h})^2 \tag{25}$$

where k_s is the shear buckling coefficient, E is the modulus of elasticity, v is the Poisson's ratio, h is the web depth, and t_w is web thickness.

3.1. Geometry and material properties

Two types of models were made: some girders unstiffened (54 cases) and the remaining (3600) girders with longitudinal stiffening, with the geometry shown in Figure 3-1. This geometry is intended to recreate the behavior of haunched girders near the supports of bridges, in which the inclined flange is under compression and the tension field is developed in the short diagonal.

In order to define the optimal position of the stiffener, it was decided to run the following positions of the stiffener:

- The stiffener height is represented as the proportion, with respect to the height of the shortest side of the girder (h_0), in which the initial position of the stiffener is established. It was stablished the values: $\frac{h_0}{4}, \frac{2h_0}{5}, \frac{h_0}{2}, \frac{3h_0}{5}$ and $\frac{3h_0}{4}$ to obtain the proportions 0.25, 0.4, 0.5, 0.6, 0.75 with respect to the total height of h_0.
- The inclination of the stiffener varies: horizontal, parallel to the inclined flange and from mid-height ($h_0/2$), to mid- height ($h_1/2$).
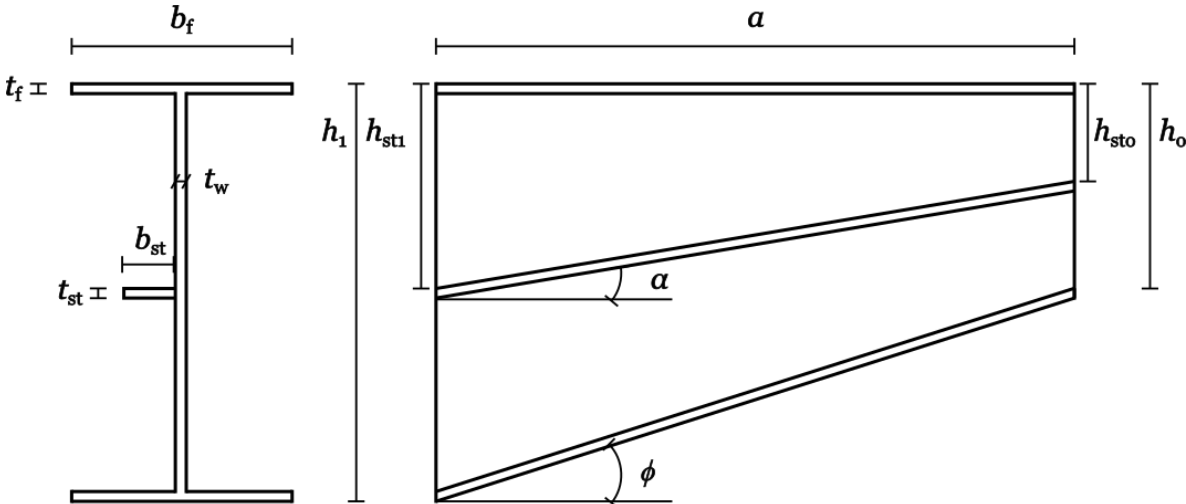
Figure 3-1. Geometry of longitudinally stiffened-haunched plate girder (Nomenclature).

All the models have the same material, structural steel, with the properties: E, the modulus of elasticity, equal to 210 GPa, and v, the Poisson's ratio, equal to 0.3.

It is also important to clarify that within the initial geometry no initial imperfection or residual stress is included, this is because the value of the critical load is a perfect (theoretical) value as explained by some authors. Faria [22] explained that initial imperfections do not diminish the critical buckling load of beams or plates. Serror [13], for his part, reported some values of results for elastic buckling with perfect plates without imperfection and neglecting the effect of residual stresses. Finally, Ferreira [19] explained that they don't include any initial geometric or material imperfection because the main aim of their study is to evaluate the effects of the critical buckling load on the locations of the longitudinal stiffeners, so it was not necessary.

3.2. Loading and boundary condition

A unit load is applied downward in the web at the higher height end, as shown in Figure 3-2. The boundary conditions are shown in Figure 3-2 and Table 3-1. With this configuration, the tension field is developed in the short diagonal and the inclined flange is under compression.
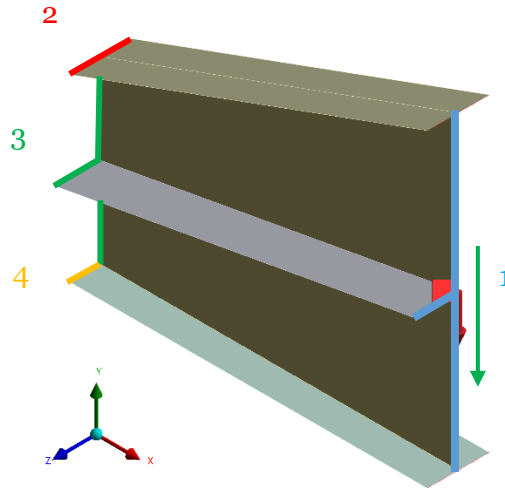
Figure 3-2. Boundary conditions and applied force.

Table 3-1. Boundary conditions.

Location							
	U_x	U_y	U_z	R_x	R_y	R_z	Force
1	F	F	R	F	F	F	$-U_y$
2	F	F	F	R	F	F	0
3	F	F	R	R	R	R	0
4	F	R	F	F	F	F	0

* F denotes free and R denotes restrained.

3.3. Mesh and analysis

A mesh convergence analysis is conducted for an unstiffened girder. The geometry of the girder is shown in Table 3-2.

Table 3-2. Geometry of girder for mesh convergence.

Property	b_f (mm)	h_0 (mm)	a (mm)	b_f (mm)	b_f (mm)	t_f (mm)	t_w (mm)
Value	180	600	800	180	800	15	3.9

Figure 3-3 presents the results of the convergence analysis. It was established a final mesh with a resolution of 25 mm because from this value there is a difference lower than 1% between the critical loads obtained.

Figure 3-3. Mesh convergence.

3.4. Verification and validation

To validate the model, experimental data found in the literature was used. The paper published by Bedynek [12] was chosen as it contains the detailed values of the geometries, the boundary conditions and the materials used in the tests carried out, as well as the critical loads obtained.

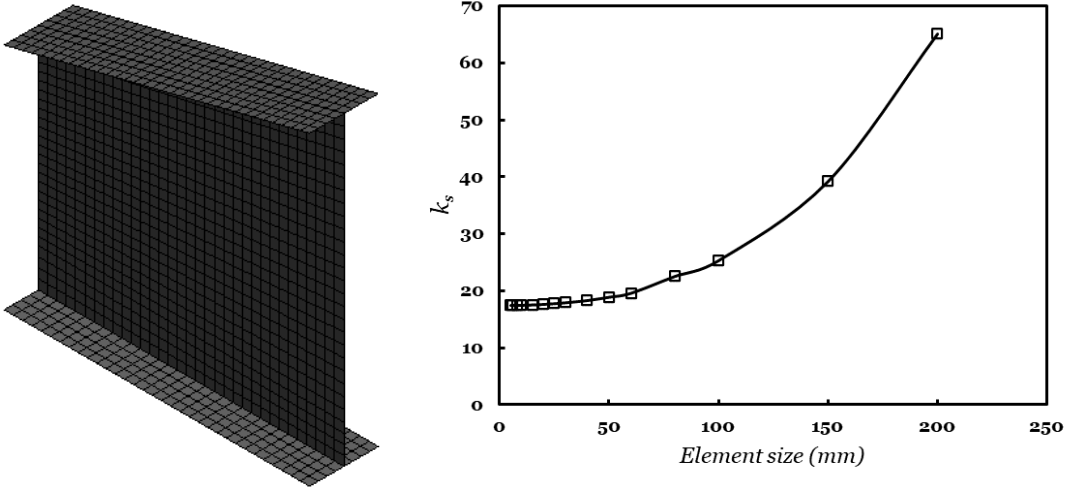The dimensions of the girders used by Bedynek [12] are presented in Table 3-3. Girder D of these tests presented in the study was not used because this girder was used to observe the shear-bending interaction.

Table 3-3. Dimensions of the tested girders for validation.

Girder	h_0 (mm)	h_1 (mm)	a (mm)	t_w (mm)	b_f (mm)	t_f (mm)	α (-)	$tan(\phi)$ (°)
A_600_800_800_4_180_15	600	800	800	4	180	15	1	0.25
B_500_800_1200_4_180_15	500	800	1200	4	180	15	1.5	0.25
C_480_800_800_4_180_15	480	800	800	4	180	15	1	0.4

The critical buckling load obtained by Bedynek [12] for each girder is presented in Table 3-3. In this table it can also be seen the critical load results obtained through FE modeling using Ansys and the percentage of difference between both values.

Table 3-4. Results of critical shear buckling load.

Girder	V_{cr} (kN) Bedynek	V_{cr} (kN) FEM	Difference
A_600_800_800_3.9_180_15	223.9	232.3	3.8%
B_500_800_1200_3.9_180_15	212	220.4	4.0%
C_480_800_800_3.9_180_15	269.1	282.5	5.0%

Since the largest difference found was 5%, it can be ensured that the model is validated and can be used later for the parametric analysis of interest.

4. Parametric study

In Table 4-1 the fixed variables and parametric ranges are presented. The reason for the chosen ranges will be explained below, in order to guarantee modeling in accordance with the reality of the use of these girders in practical design.

Table 4-1. Parameters.

Dimension	Value
h_0 (mm)	1000
b_f	$h_1/6$
ϕ (°)	0, 10, 15, 20, 25, 30
a/h_0	1, 2, 3
t_f/t_w	2, 3, 4
γ_s	0, 5, 10, 20, 50, 150
Stiffener height (proportion of h_0)	0.25, 0.4, 0.5, 0.6, 0.75
Stiffener position	Horizontal, Inclined, Mid-height

- Web depth (D): The depth D (in this thesis h_0 and h_1) was fixed by Lee [10] in his model at 40 inches (1016 mm), functioning as standard measure. Despite this value is fixed, the other parameters are applied in ratio forms, allowing for the accommodation of web plate depths differing from the standard 40 inches. This approach ensures that the results apply to a vast range of practical designs, thus enhancing the model's versatility and utility.

- Flange Width (b_f): In accordance with the guidelines provided by AASHTO [23], the minimum flange proportion for I-sections stipulates that the flange width (b_f) should be no less than a sixth of the web depth ($b_f \geq D/6$). D is considered as the larger plate width h_1 in this study (Ibrahim [14]). This criterion ensures that the flange dimensions are appropriately scaled to the web depth, promoting structural integrity and efficiency.

- Inclination angle ($\phi°$): Following the recommendations by Mirambell [11], the inclination angle ranges between 5.7° and 30.9°. However, to simplify the model and adhere to practical design considerations, angles were normalized to integer multiples of 5°, provided they exceed a 10° inclination. This modification narrows the range to between 10° and 30°, which remains sufficiently comprehensive while facilitating ease of design and analysis.

- Aspect Ratio (a/h_0): Following the work of Lee et al. [24], the model adopts an aspect ratio (a/h_0) range of 0.5 to 3. To streamline the analysis, only integer

values within this range were considered (i.e., 1, 2, and 3), aligning with practical design scenarios and simplifying the computational process.

- Thickness Ratio (t_f/t_w): As Serror [13] made, the thickness ratio of the flange to the web spans from 2 to 4. In this model it was considered inclusively the intermediate value of 3. This range encompasses the typical proportions encountered in structural elements, ensuring that the model reflects real-world design practices.

- Relative Flexural Rigidity (γ_s): The model employs a relative flexural rigidity range from 0 to 150, as initially proposed by Maiorana et al. [25]. This spectrum allows for the examination of various stiffness scenarios, bringing to an extensive range of structural configurations.

- Stiffener height and position: The selection criteria for stiffener height and position were established to cover a wide spectrum of values, thereby affording a comprehensive analysis of stiffener effectiveness across different structural scenarios.

In summary, the selection and justification of these parameters are grounded in established research and industry standards, aiming to ensure that the model's applicability and relevance extend to a broad spectrum of structural design challenges. By employing ratios and standardized ranges, the model achieves a balance between specificity and versatility, making it a robust tool for analyzing plate girders under various configurations and conditions.

5. Stiffener placement and influence of parameters.

5.1. Stiffener placement

The first result presented pertains to stiffener placement. The position of the stiffener that increases the resistance the most (compared to unstiffened cases) corresponds to the position parallel to the inclined flange, resulting in an average resistance increase of 186%, as illustrated in Figure 5-1. The horizontal stiffening case increases the resistance by 67% and the stiffening at the middle of each height by 128%, both with respect to the non-stiffened cases. This shows that any type of longitudinal stiffening automatically increases the resistance of said girders and improves their working conditions.
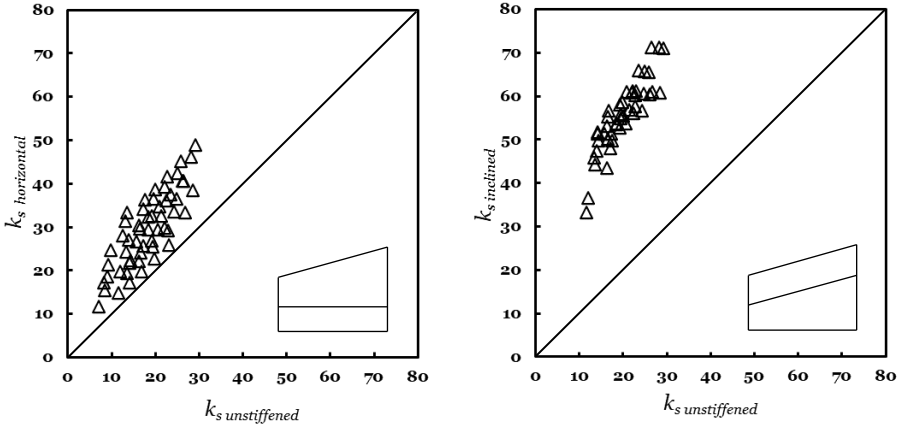
(a) Horizontal stiffener.

(b) Inclined stiffener.
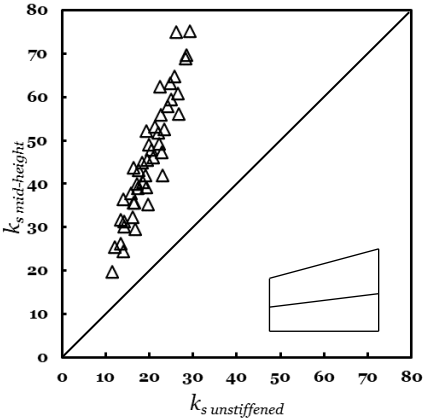
(c) Mid-Height stiffener.

Figure 5-1. Influence of stiffening.

However, it would not be correct to establish the position parallel to the inclined flange as the optimal position yet. This is because, as explained previously, only these stiffening results have been analyzed compared with the 54 cases that were not stiffened. This chapter will go into more detail about the optimal position of a single longitudinal stiffener, in addition to the influence of the varied geometric parameters with respect to k_s.

First, a plot of the average of the shear buckling coefficient, discriminating by the flexural stiffness, against the position of the stiffener with respect to the lower height (called stiffener height), was made. This was done for all the stiffened cases available results (3600 cases).

It is evident in Figure 5-2 that as the flexural rigidity increases, the average of k_s increases. Furthermore, there is an increase in said value between the positions $0.5h_0$ and $0.6h_0$. As the stiffener moves toward the ends, closer to the flanges, the lower values of k_s occurs.
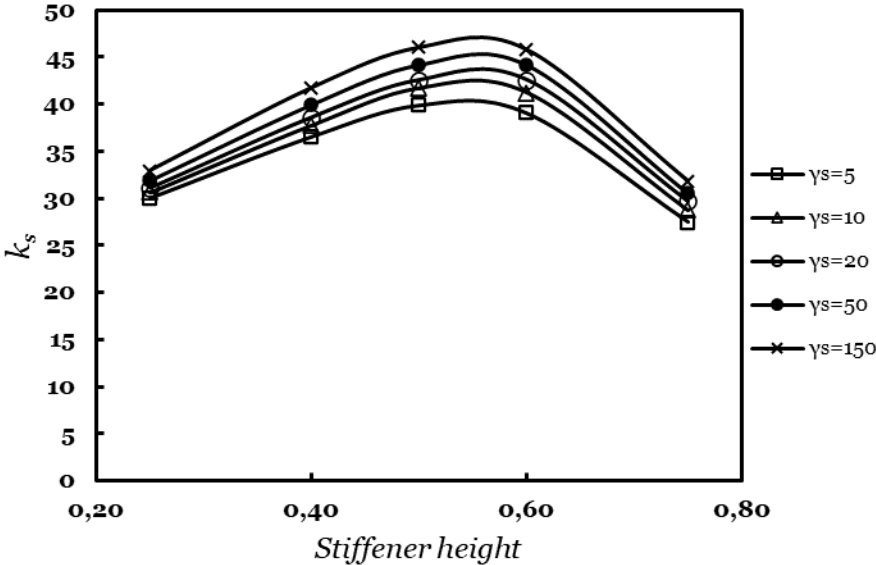
Figure 5-2. Stiffener height compared with k_s.

On the other hand, the same was done with the three possible positions of the stiffener (horizontal, parallel to the inclined flange -just called inclined here- and from half of one height to half of the other- just mid-height here-). In Figure 5-3 the obtained results are shown. It can be seen in this figure that the highest values of the buckling coefficient k_s are found for the mid-height position. Being greater in ascending order according to the flexural rigidity of the stiffener. The lowest values of k_s are found for the horizontal position.
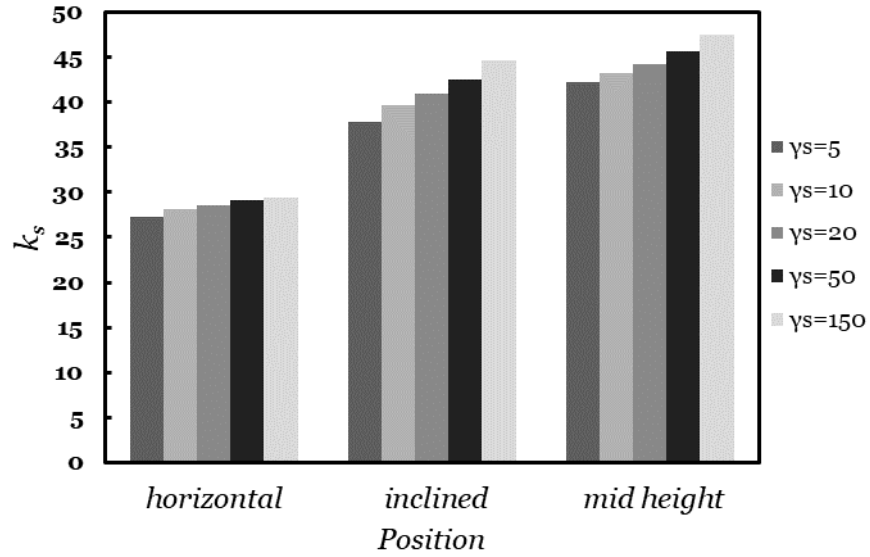
Figure 5-3. Position of the stiffener compared with k_s.

However, to make a fair comparison between the inclined position and the mid-height position, the behavior of k_s was plotted against the variable stiffener height, which, as explained before, is a measure of the proportion of the location of the stiffener with respect to the shortest side. This was done because what is shown in Figure 5-3 is an average of the stiffener heights, therefore, it is not evident which of these presents the most optimal behavior. This graph is shown in Figure 5-4 (it is just for the inclined case).
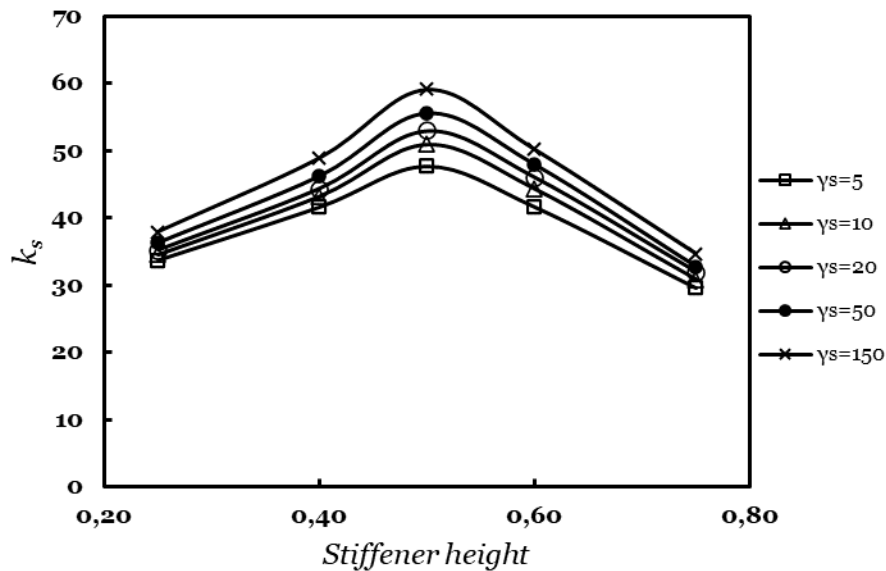

Figure 5-4. Stiffener height compared with k_s for inclined position.

It is thus evident that the optimal position is to locate the stiffener at half the height with respect to h_0. Finally, all that remains is to compare the positions: inclined with a stiffener height equal to 0.5 against the mid-height position. Although these two sound similar, the mid height position forces the stiffener to be located in the middle of the height h_1, while the inclined position allows it to reach a different point than the middle one.

A graph to compare both positions was made in Figure 5-5. It is seen in this figure that for both cases the ranges are very similar (ranging between $k_s = 40 - 60$). Being practical, the mid height position is the one that allows more facility when designing. On the other hand, the inclined position with a stiffener height equal to 0.5 has an average of k_s that is slightly higher than the mid height case. For these reasons and being objective (as it is known that they are numerical values), both positions will be considered as the optimal position.

This leaves us that the optimal position in this thesis will be considered as:

- The stiffener is located at half the height with respect to the h_0 side.

- For side h_1 the position of the stiffener can vary between: the middle of the side (mid height position) and another position as indicated by the inclination of the stiffener (inclined position with stiffener height equal to 0.5).
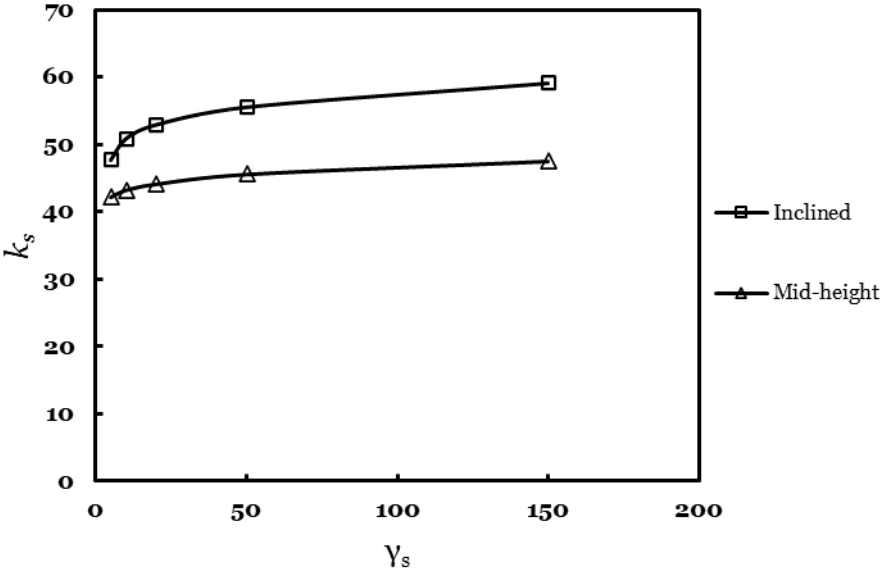

Figure 5-5. Values of k_s for inclined with stiffener height 0.5 and mid height.

This conclusion is in accordance with what is found in the literature regarding to the optimal position of a longitudinal stiffener. For example, Bedynek in his Doctoral Thesis

[26] explained that for the case of longitudinally stiffened tapered steel plate girders mainly subjected to shear, an inclined position of the stiffener connecting the two points at the mid-heights of both depths is the most favorable position. However, as is shown in Figure 5-6, he did not analyze the case of locating the stiffener at half a height and having it inclined to connect with the other height (he only has it horizontal as evidenced in cases I and III).
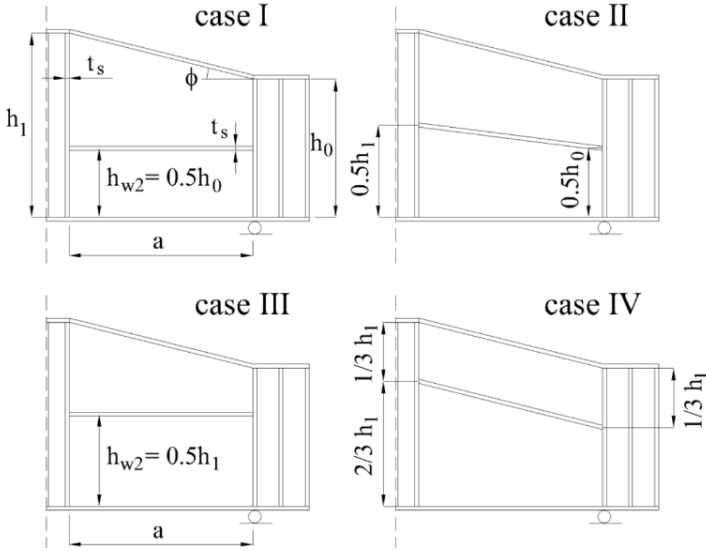
Figure 5-6. Four popular cases of position of the longitudinal stiffener [26]**.**

On the other hand, Estrada et al. [18] and Ferreira [19] also reached similar conclusions: the optimum position of a stiffener b/d is always found when the stiffener can divide the plates in equal subpanels, which means that, for plate web subjected mainly to shear, when the two resulting subpanels buckle simultaneously (if bending effects are not considered). However, these last two only analyzed horizontal stiffeners, so they omitted to analyze what would happen if it were inclined.

5.2. Influence of the stiffener position and flexural rigidity γ_s

The stiffener flexural rigidity is defined as:

$$\gamma_s = \frac{E * I_{st}}{h_w * D} = \frac{10.9 * I_{st}}{h_w * t_w{}^3} \tag{26}$$

where I_{st} is the second moment of area of the stiffener respect to an axis placed at the centroid of the area including the stiffener and a portion of the web of $15t_w$ on each side as defined by the Eurocode [15]. This code also states that when calculating the shear buckling coefficient k_s, the value of the second moment of area must be divided by three.

41

(a) ϕ=10°.

(b) ϕ=15°.

(c) ϕ=20°.

(d) ϕ=25°.
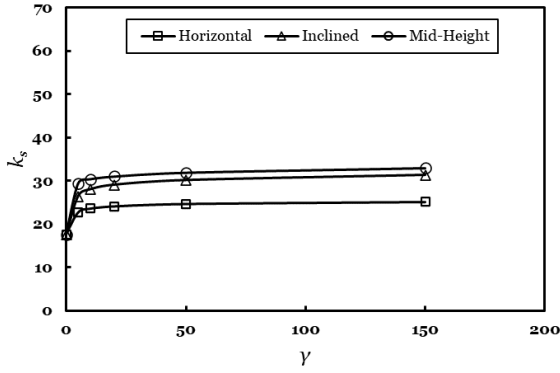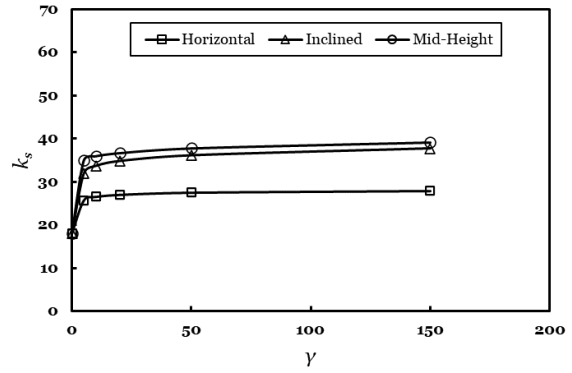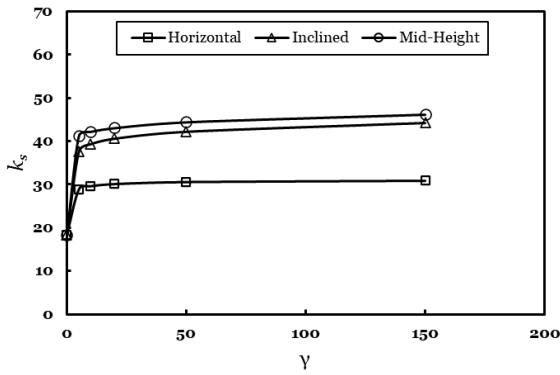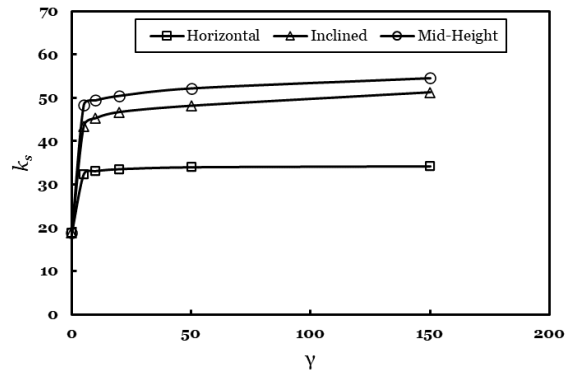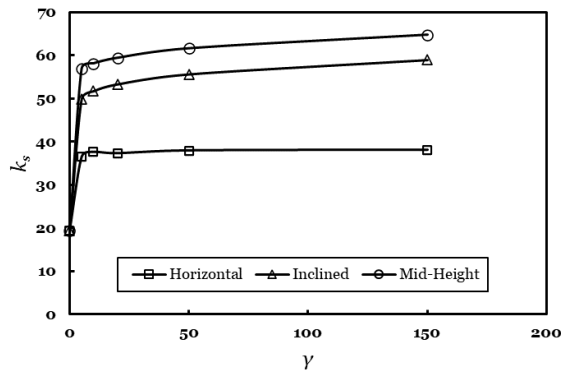
(e) ϕ=30°.

Figure 5-7. k_s in terms of γ_s.

Figure 5-7 shows the variation of the buckling coefficient k_s in terms of γ_s. The main analysis is that after a reaching a certain value of γ_s, there is not a significant increase of the value of k_s. This value is the transition between the behavior of a weak stiffener and the

behavior of a strong stiffener. As presented in the next plots, the value of minimum rigidity for a strong stiffener is $\gamma_s = 20$. After this value the buckling coefficient remains almost constant, therefore the conclusion is that for a strong stiffener, there is a diminished influence of the flexural rigidity on the value of k_s.

This difference between strong and weak stiffeners will be crucial in determining the buckling mode of the girder, as Alinia [20] explains:

- Using flexible stiffeners: In this case the stiffeners do buckle and deform together with the plate as a unit, otherwise known as the overall buckling mode. Here, the buckling stress increases; the amount of which depends on the rigidity of the stiffeners. However, the buckling mode of plate does not change in comparison to the unstiffened plate.
- Using rigid stiffeners: In this case the stiffeners do not buckle nor deform together with the plate, but by undergoing a large amount of twist, actually divide the width of the plate into sub-panels, and finally change the buckling mode, otherwise known as the local buckling mode. Here, the increase in the buckling stress is due to the reduced width of panels.

5.3. Influence of the web slenderness h_1/t_w

Also known as slenderness ratio, it was demonstrated at Rico 2023 [27] that the slenderness parameter h_1/t_w has a diminished impact on the shear buckling coefficient, as long as the web is slender $\frac{h_1}{t_w} > 150$ and the code limit is maintained $\frac{h_1}{t_w} < 300$ [23]. For this reason, the following results will not include the aforementioned parameter.

This behavior can be explained because shear buckling is more influenced by the web's ability to transfer shear forces through the thickness of the material, and not so much by the slenderness ratio of the web. Furthermore, the stiffness provided by longitudinal stiffeners helps distribute shear forces and minimize the risk of localized buckling, which may explain the lack of direct influence of web slenderness on shear buckling. However, this is a variable of great relevance to study the ultimate shear load, since the longitudinal stiffeners increase the resistance to local buckling of the web, but the slenderness of the web continues to be a critical factor in determining the overall strength and stiffness of the girder, thus affecting the ultimate load.

5.4. Influence of the thickness ratio t_f/t_w

In Figure 5-8 to Figure 5-10 the variation of buckling coefficient k_s in terms of t_f/t_w is shown.

(a) $a/h_0 = 1$, ф=10°.

(b) $a/h_0 = 1$, ф $= 15$°.

(c) $a/h_0 = 1$, ф=20°.

(d) $a/h_0 = 1$, ф $= 25$°.

(e) $a/h_0 = 1$, ф=30°.
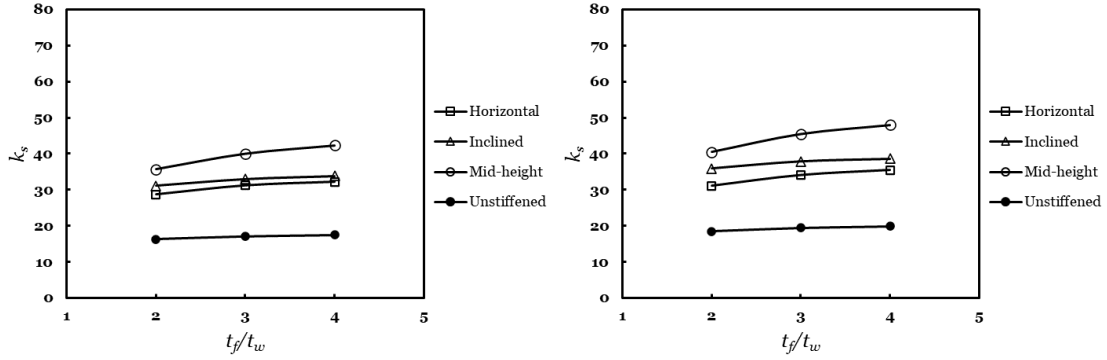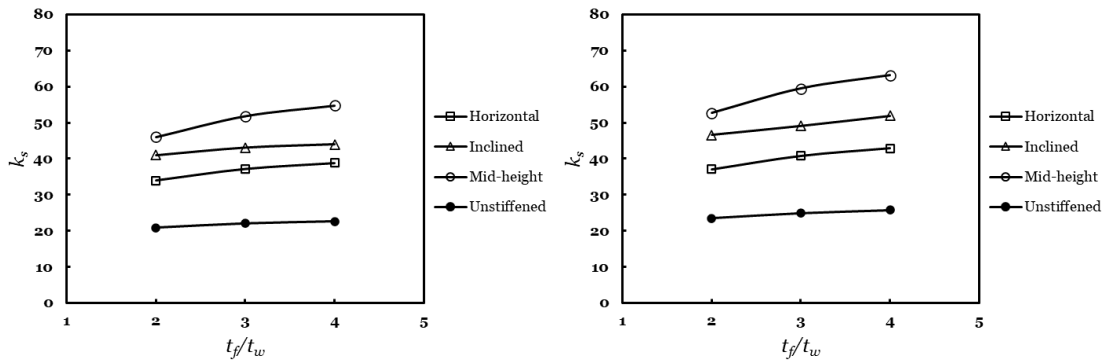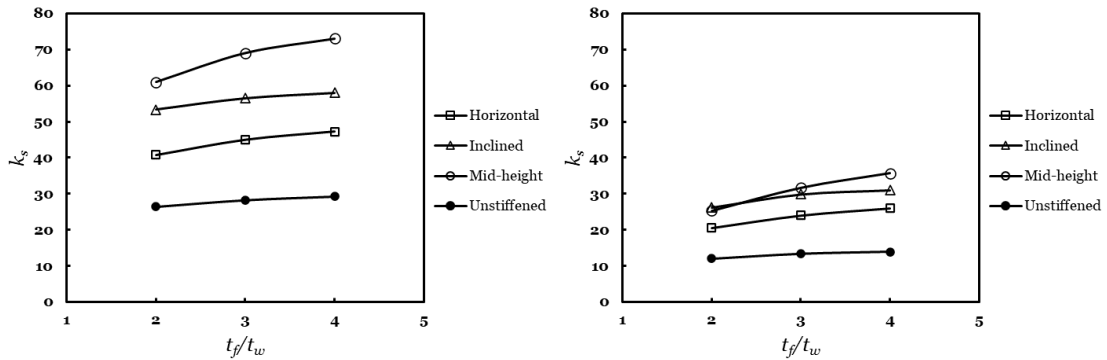
(f) $a/h_0 = 2$, ф $= 10$°.

Figure 5-8. Buckling coefficients k_s in terms of t_f/t_w for $\gamma_s = 50$.

(g) $a/h_0 = 2$, ф=15°.

(h) $a/h_0 = 2$, ф $= 20°$.

(i) $a/h_0 = 2$, ф=25°.

(j) $a/h_0 = 2$, ф $= 30°$.

(k) $a/h_0 = 3$, ф=10°.
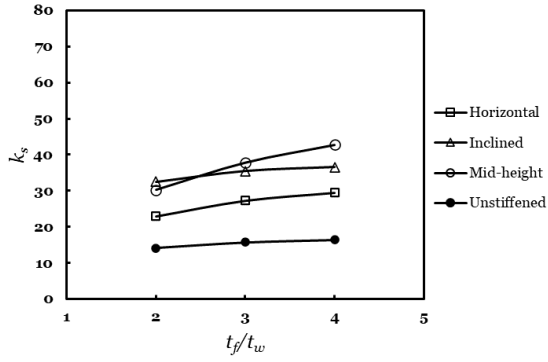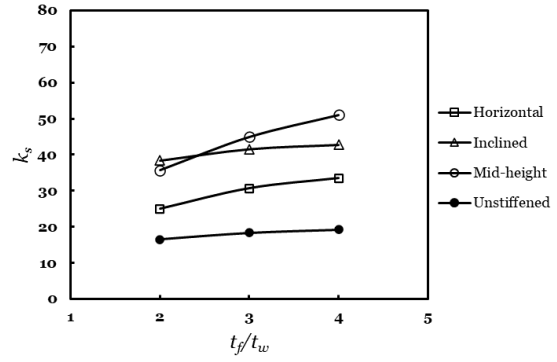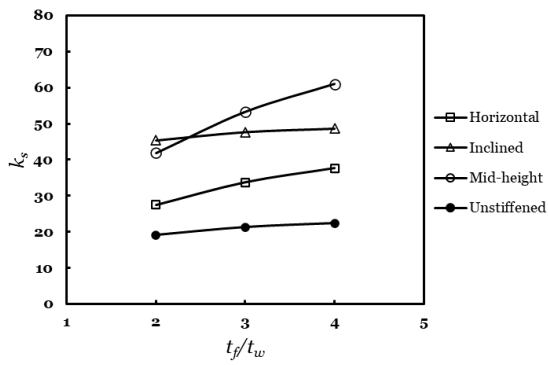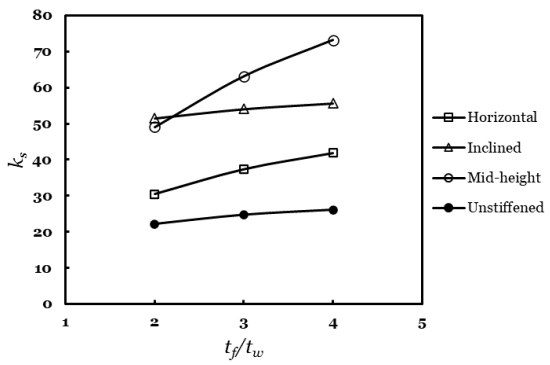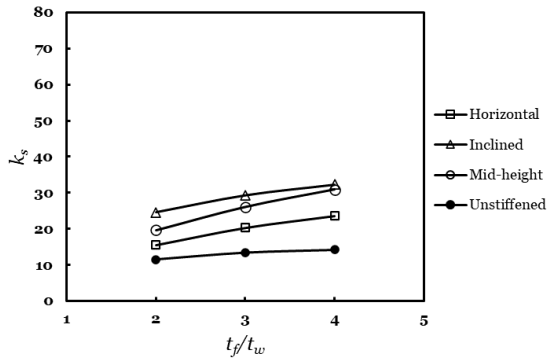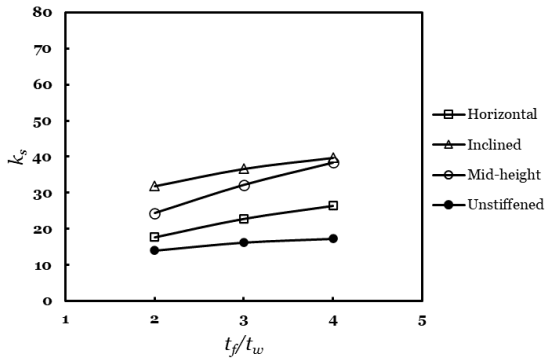
(l) $a/h_0 = 3$, ф $= 15°$.

Figure 5-9. Buckling coefficients k_s in terms of t_f/t_w for $\gamma_s = 50$.

(m) $a/h_0 = 3$, ɸ=20°.

(n) $a/h_0 = 3$, ɸ $= 25°$.
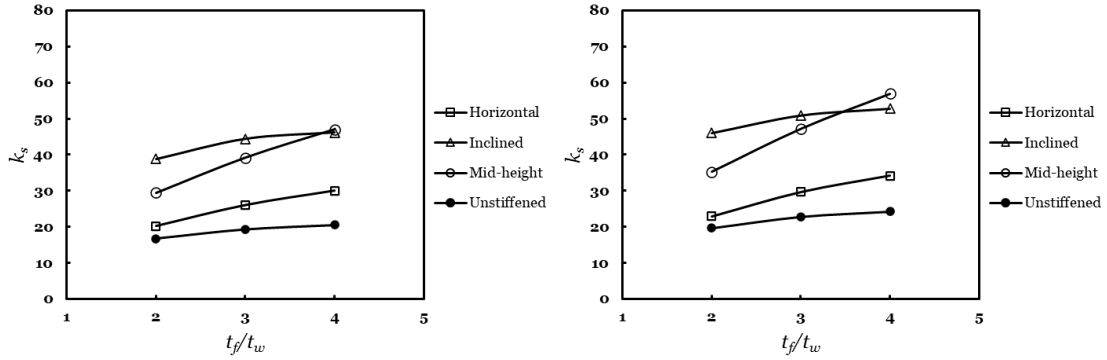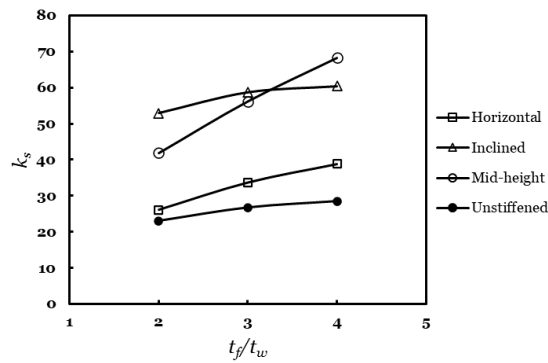
(o) $a/h_0 = 3$, ɸ=30°.

Figure 5-10. Buckling coefficients k_s in terms of t_f/t_w for $\gamma_s = 50$.

It is observed that for all cases, there is an increase in the buckling coefficient as the flange-to-web thickness ratio is greater. This is expected, as the thickness of the flanges increase, the boundary condition of the web to flange juncture approaches to a fixed support, thus increasing the rigidity and the shear buckling capacity of the girder. As the variation of this ratio makes the buckling coefficient change, this value is included in the analysis.

5.5. Influence of the panel aspect ratio a/h_0

In Figure 5-11 to Figure 5-13 the variation of the buckling coefficient k_s in terms of the aspect ratio a/h_0 is presented.

46
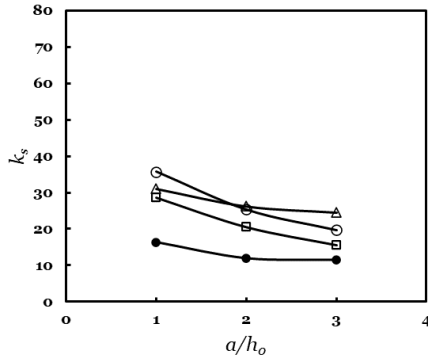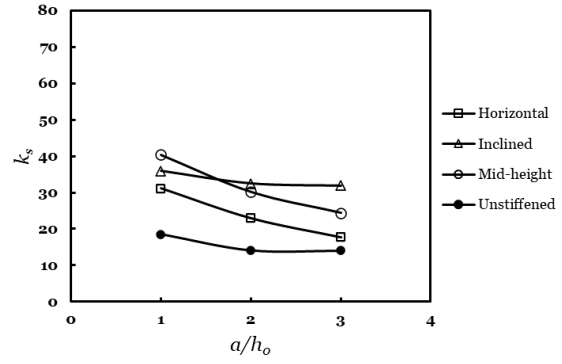
(a) $t_f/t_w = 2$, $\phi=10°$.

(b) $t_f/t_w = 2$, $\phi = 15°$.
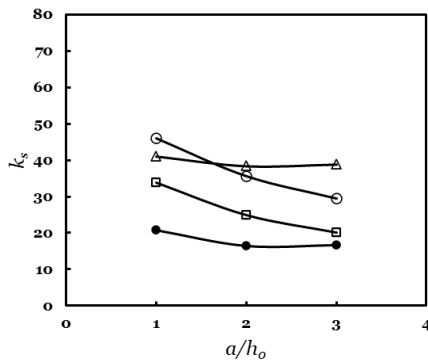
(c) $t_f/t_w = 2$, $\phi=20°$.
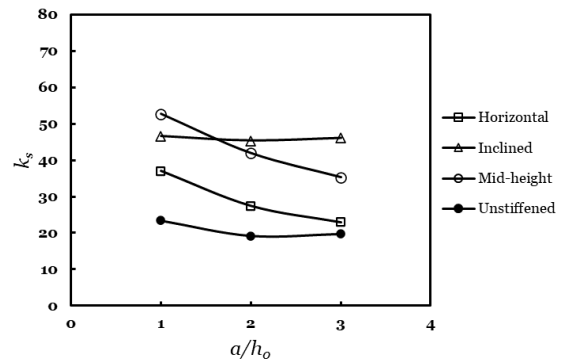
(d) $t_f/t_w = 2$, $\phi = 25°$.
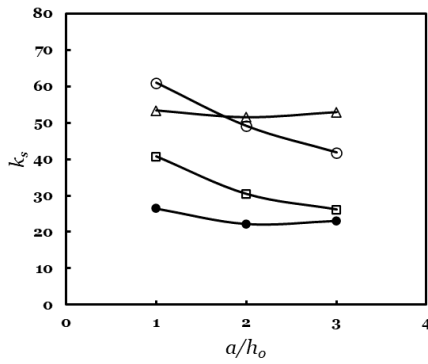
(e) $t_f/t_w = 2$, $\phi=30°$.
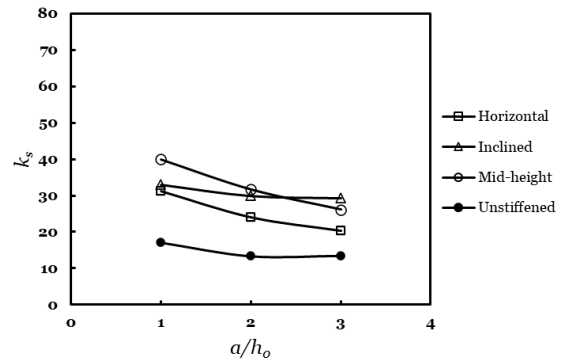
(f) $t_f/t_w = 3$, $\phi = 10°$.

Figure 5-11. Buckling coefficients k_s in terms of a/h_0 for $\gamma_s = 50$.

(g) $t_f/t_w = 3$, ф=15°.

(h) $t_f/t_w = 3$, ф $= 20°$.

(i) $t_f/t_w = 3$, ф=25°.

(j) $t_f/t_w = 3$, ф $= 30°$.

(k) $t_f/t_w = 4$, ф=10°.
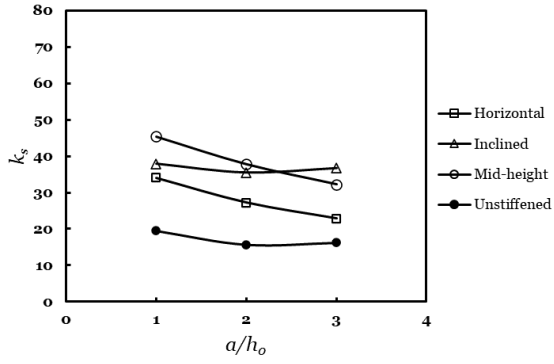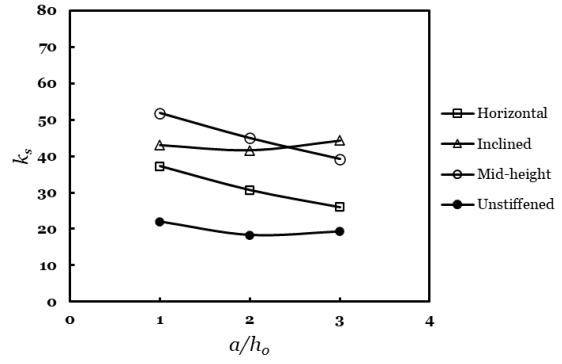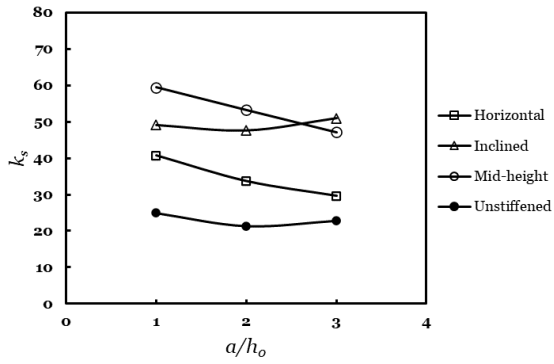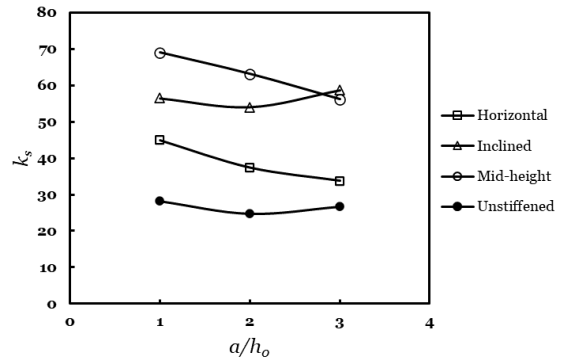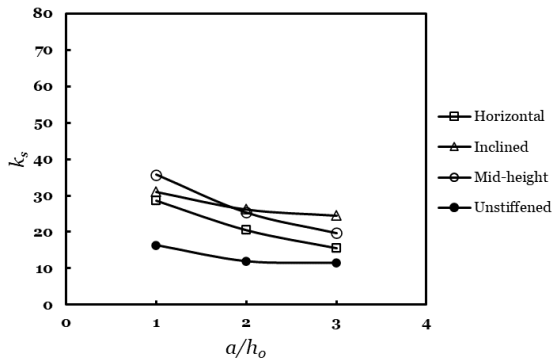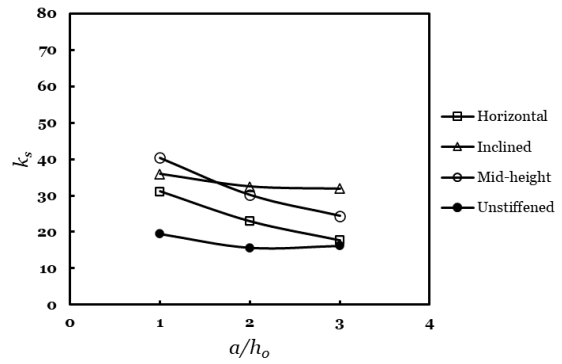
(l) $t_f/t_w = 4$, ф $= 15°$.

Figure 5-12. Buckling coefficients k_s in terms of a/h_0 for $\gamma_s = 50$.
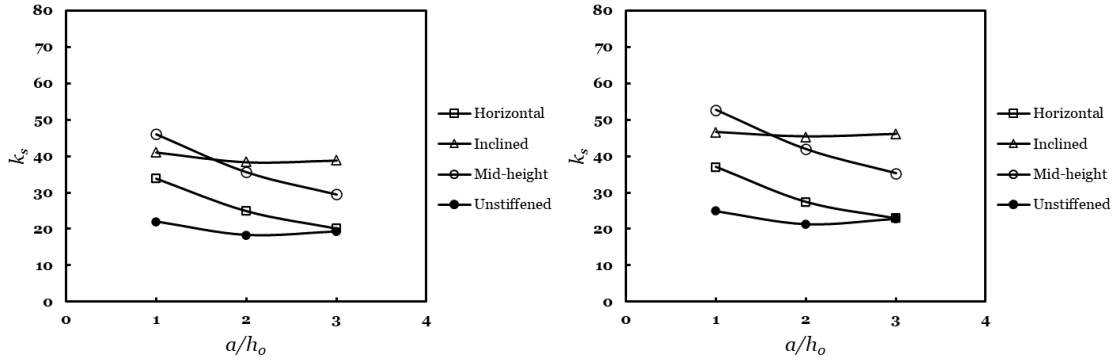
(m) $t_f/t_w = 4, \phi=20°$.

(n) $t_f/t_w = 4, \phi = 25°$.
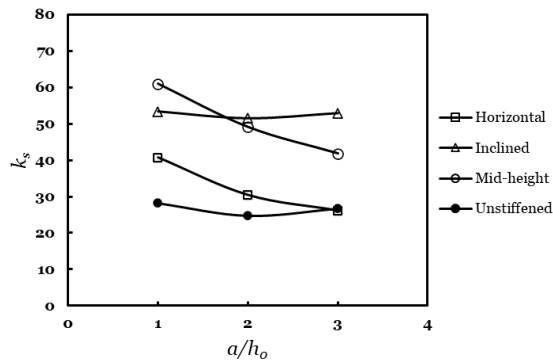
(o) $t_f/t_w = 4, \phi=30°$.

Figure 5-13. Buckling coefficients k_s in terms of a/h_0 for $\gamma_s = 50$.

It is observed that for all cases, as the aspect ratio increases, the buckling coefficient decreases. This is explained because as the panel aspect ratio increases, the panel is longer and bending stresses increase, thus reducing the shear buckling capacity. As this parameter makes the buckling coefficient change, this value must be included in the analysis.

5.6. Influence of the haunch inclination tan(ϕ)

In Figure 5-13 to Figure 5-15 the variation of the buckling coefficient k_s in terms of the haunch inclination tan(ϕ) is presented.
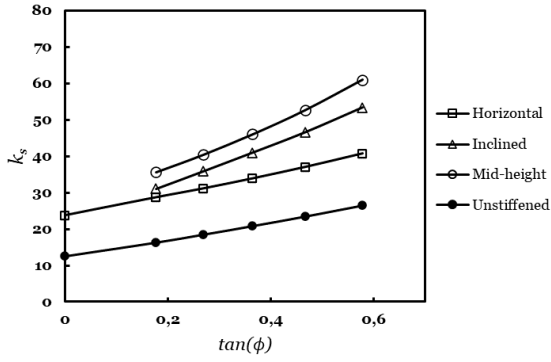
(a) $a/h_0 = 1, t_f/t_w = 2.$
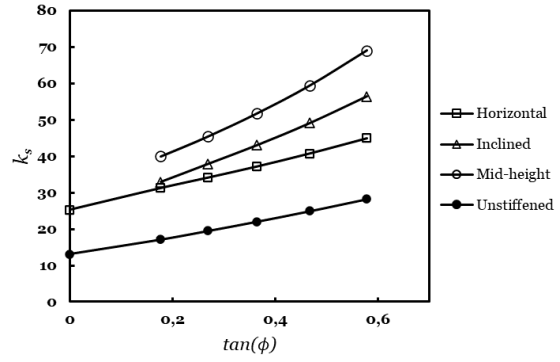
(b) $a/h_0 = 1, t_f/t_w = 3.$
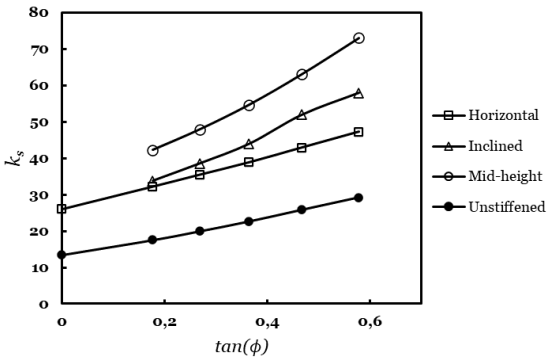
(c) $a/h_0 = 1, t_f/t_w = 4.$
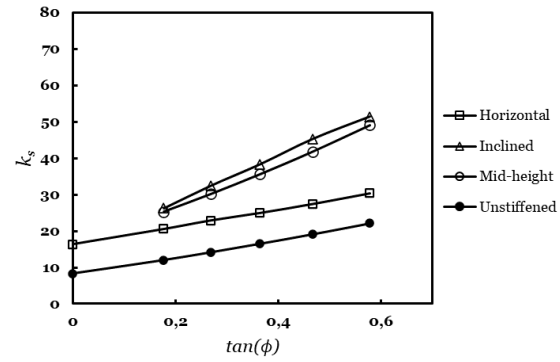
(d) $a/h_0 = 2, t_f/t_w = 2.$
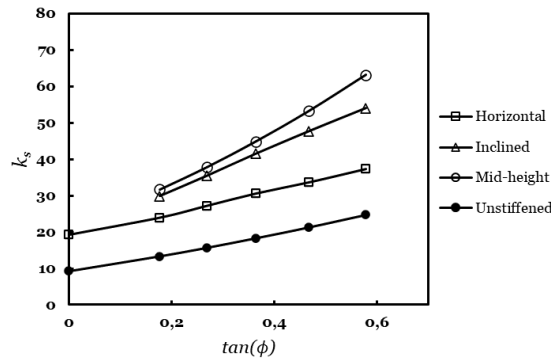
(e) $a/h_0 = 2, t_f/t_w = 3.$
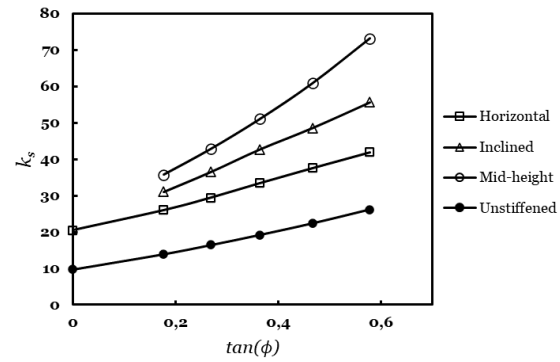
(f) $a/h_0 = 2, t_f/t_w = 4.$

Figure 5-14. Buckling coefficients k_s in terms of $tan(\phi)$ for $\gamma_s = 50$.
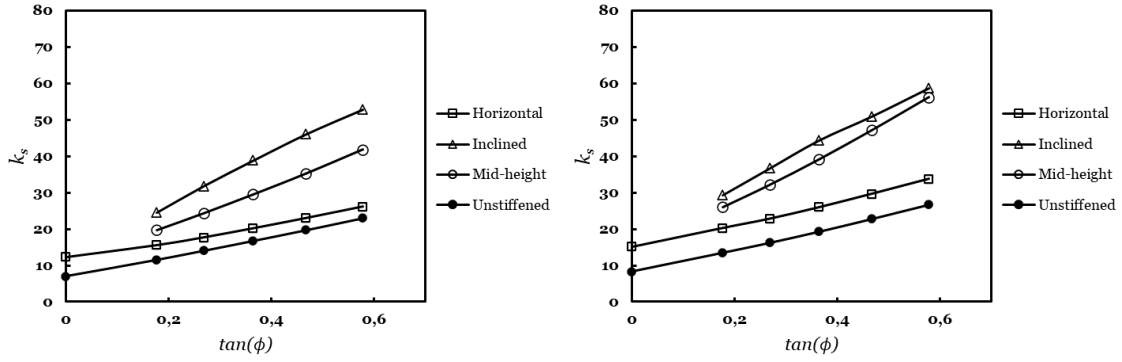
(g) $a/h_0 = 3, t_f/t_w = 2.$

(h) $a/h_0 = 3, t_f/t_w = 3.$
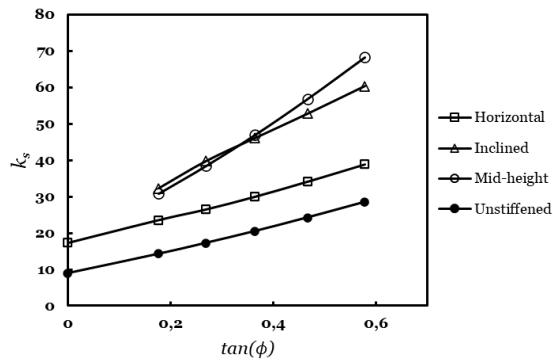
(i) $a/h_0 = 3, t_f/t_w = 4.$
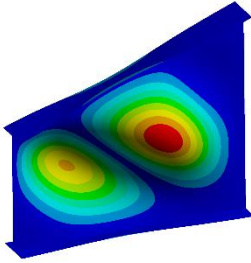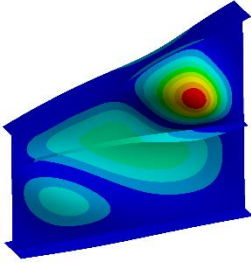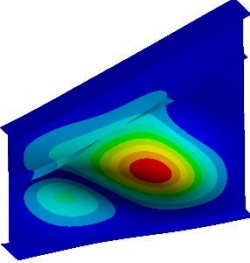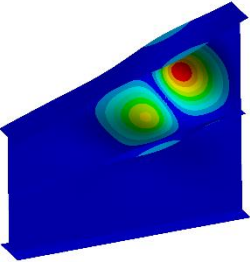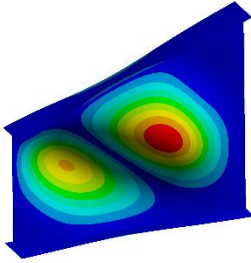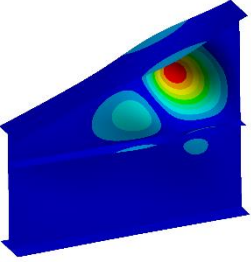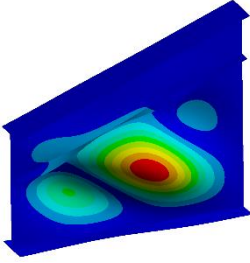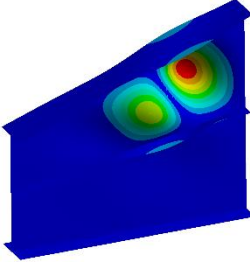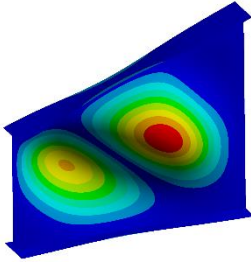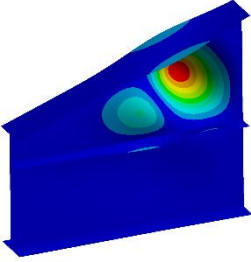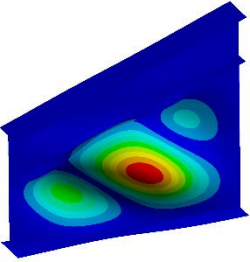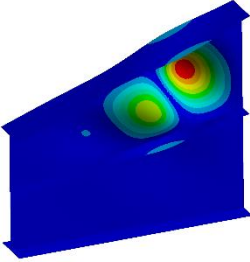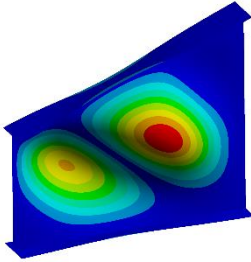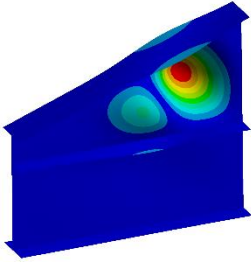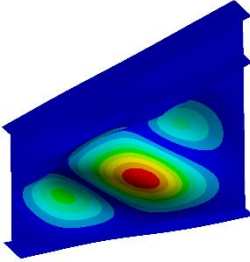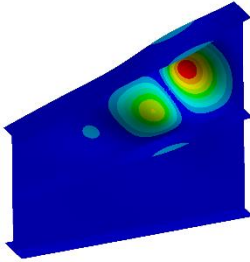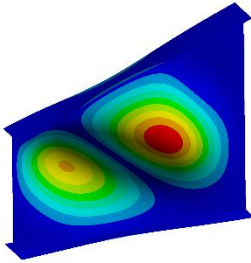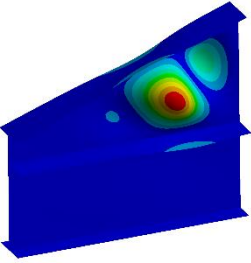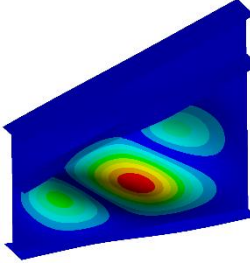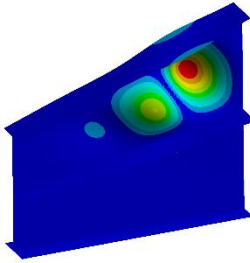
Figure 5-15. Buckling coefficients k_s in terms of $tan(\phi)$ for $\gamma_s = 50$.

It is observed that for all cases, as the haunch angle ϕ increases the buckling coefficient also increases. As this parameter affects the buckling coefficient, this value must be included in the analysis.

5.7. Buckling shapes

Table 5-1 shows the buckling shapes, varying the stiffener rigidity and position, for a girder with a/h_o=2, t_f/t_w=2, $\phi = 20°$.

Table 5-1. Buckling shapes for $a/h_0 = 2, t_f/t_w = 2, \phi = 20°$.

γ_s	Stiffener position			
	Unstiffened	Horizontal	Inclined	Mid-height
5	$k_s = 16.54$	$k_s = 31.1$	$k_s = 34.91$	$k_s = 33.51$
10	$k_s = 16.54$	$k_s = 32.33$	$k_s = 37.59$	$k_s = 34..1$
20	$k_s = 16.54$	$k_s = 32.84$	$k_s = 39.48$	$k_s = 34.68$
50	$k_s = 16.54$	$k_s = 33.42$	$k_s = 41.55$	$k_s = 35.67$
150	$k_s = 16.54$	$k_s = 33.93$	$k_s = 44.03$	$k_s = 37.06$

Observing the deformed shapes in Table 5-1, the following findings are highlighted:

1. When the panel is unstiffened $\gamma_s = 0$, the buckling shape involves the whole web panel, thus reducing the capacity ($k_s = 16.54$).

2. When the stiffener is weak $\gamma_s = 5\text{-}10$, the stiffener does not provide a nodal line of near zero out-of-plane displacements, and the buckling also involves the whole web panel and the stiffener. Nevertheless, the buckling coefficient k_s increases compared to the unstiffened girder.

3. When the stiffener is strong, $\gamma_s = 20$, buckling occurs only on one sub-panel, as the stiffener restricts the out-of-plane displacement similar to a nodal line with near zero displacements, thus dividing the whole web panel into two sub-panels, and increasing the capacity of the girder to resisting shear buckling. For $\gamma_s = 50$ and $\gamma_s = 150$ the difference in the buckling coefficient is very small compared to that obtained for a stiffener with $\gamma_s = 20$.

6. Proposal of buckling coefficient

The DataRobot software [28], enhanced with the Eureqa Models extension, was used to discover the equation that best predicts the behavior of the buckling coefficient under shear loading as a function of the variables: aspect ratio, thickness ratio and haunch inclination.

This tool provides a portal to a suite of model blueprints specifically designed for various tasks: Eureqa Generalized Additive Models (Eureqa GAM), Eureqa Regression, and Eureqa Classification Models. These models are the product of Eureqa's advanced machine learning algorithm, which is engineered to strike an optimal balance between model complexity and predictive accuracy. This balance is crucial, as overly complex models may overfit the data (and start being unpractical), while overly simple models might underperform in predictive tasks.

The step-by-step procedure used and the justification of the variables used are below:

1. Selection of the target variable: The initial step involves choosing the target variable, in this instance denoted as k_s. This choice is fundamental, as it determines the focus of the modeling effort and guides the subsequent steps in the process.

2. Choice of modeling mode: The decision to utilize the 'integral autopilot mode' is strategic, driven by the objective of maximizing the model's precision. This model is distinguished by its comprehensive and automated search for the optimal model, thereby facilitating a more efficient modeling process.

3. Exclusion of time-based modeling: Given the absence of temporal elements in the dataset, time-based modeling is not selected. This decision underscores the importance of aligning the modeling approach with the nature of the data, ensuring that the model complexity does not escalate unnecessarily.

4. Adoption of the Eureqa Regressor model: It is decided to use the Eureqa Regressor model with a default configuration of 3000 generations. This model dynamically refines the coefficients of previously derived solutions, improving the adaptability and accuracy of the model with each iteration.

5. Data splitting strategy: 64% of the data set is allocated for training purposes and the rest is left for validation data. This split ensures that the model is not only well-trained but also able to generalize its predictions beyond the training data set.

The architecture of Machine Learning is summarized in Figure 6-1:
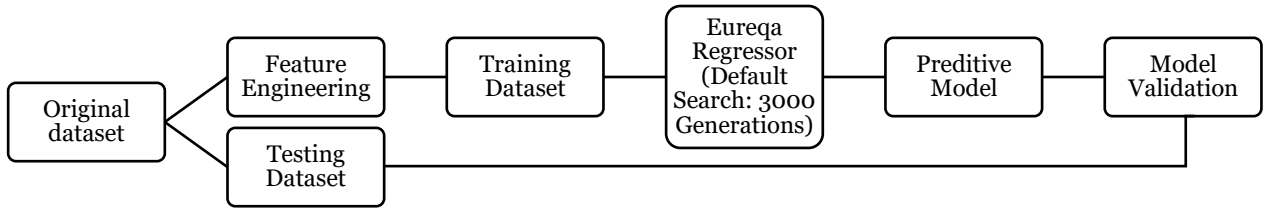
Figure 6-1. Machine learning architecture.

Now, the Eureqa algorithm was used to determine two equations:

- A better equation for the buckling coefficients k_s for unstiffened girders. The explanation for this is below.

- An equation to calculate the buckling coefficient k_s for longitudinal stiffened cases only for the optimal position since it is the focus of practical engineering.

The reason for proposing a modified equation for unstiffened girders is to obtain a more economical design. The equation for unstiffened girders proposed by Timoshenko [5], in this thesis Eq. (4), is very conservative because it was calculated using simply supported plates. An example of this can be seen in Figure 6-2, in which it can be seen that the values obtained with the equation proposed when divided by the values obtained through numerical modeling are coefficients less than unity, so despite that the original equation is on the safe side, it is too conservative in arriving at values of 0.2 and 0.3.
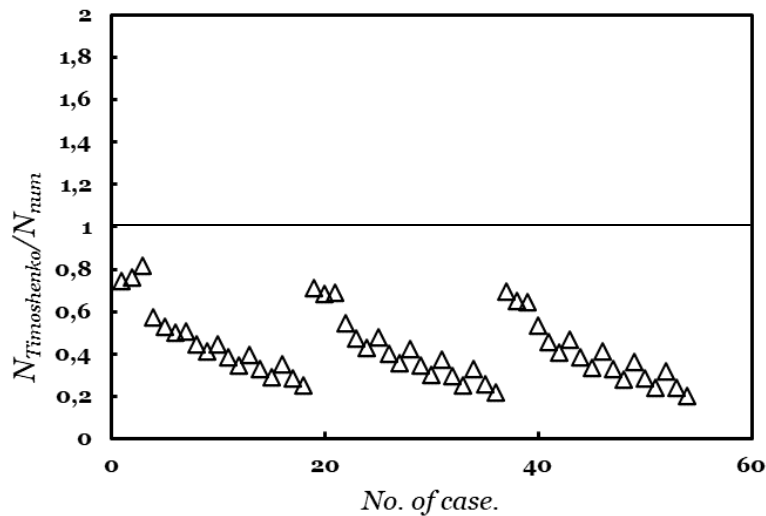
Figure 6-2. Comparison between [5] and numerical results.

This is why it was decided, through the use of machine learning, to improve the equation that is classically found in the literature, where:

$$k_\tau = 5.34 + 4.00 * \left(\frac{h_w}{a}\right)^2 \tag{27}$$

An increase in the value of the buckling coefficient is then proposed by adding two fundamental values: the influence of the variable haunch inclination and thickness ratio, , that was shown both are fundamental variables that influence the k_s value ,thus finding that:

$$k_{uns} = k_\tau + 28 * \tan(\phi) + \left(\frac{t_f}{t_w}\right) \tag{28}$$

Now, for the case with stiffener, comparative graphs were also made against other famous proposed equations. In Figure 6-3 it can be seen the relation between values obtained with the equation proposed by Bedynek [12] for typology I, in this thesis Eq. (11), when divided by the values obtained through numerical modeling coefficients are between 0.2 and 0.4. The reason is that the equation proposed by Bedynek does not include any longitudinal stiffener that increases the value of k_s.
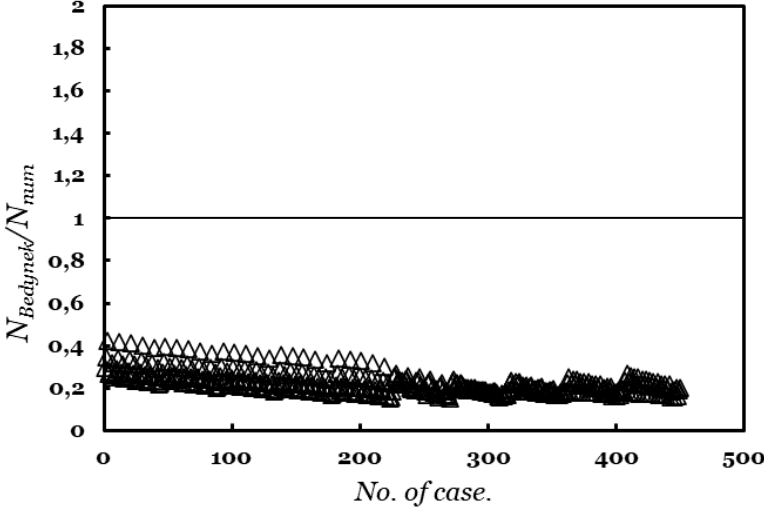
Figure 6-3. Comparison between [12] and numerical results.

The same was done with the equation proposed by the Eurocode EC3: 1-5 [15], for the case of a longitudinal stiffener and an aspect ratio greater than 3. It is observed in the comparison that they are still very conservative values, so it is necessary to create other types of equations for these cases.
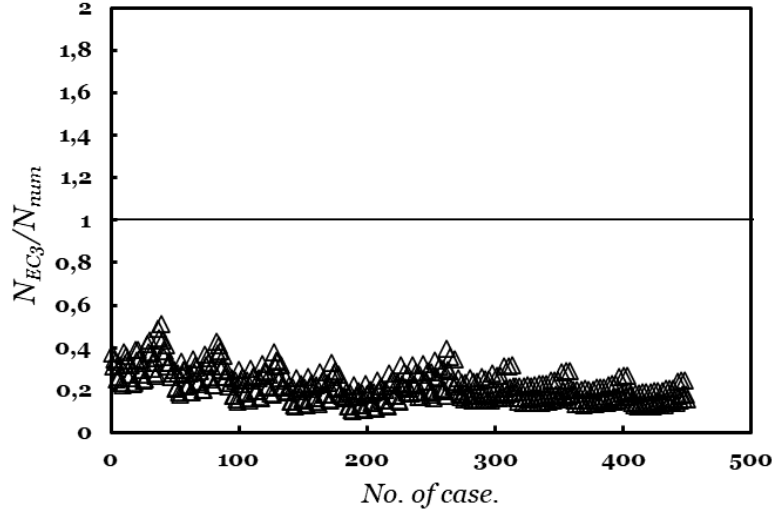
Figure 6-4. Comparison between [15] and numerical results.

Hence the equation that was the main objective of this thesis is proposed now: an equation to determine the shear buckling coefficient for longitudinally stiffened beams. The reader is reminded that only the equation for the optimal position already defined in this thesis is valid. For this, the Höglund [17] equation was taken as the base equation, which was for a single half-height to half-height stiffener, which was defined as:

$$k_H = 5.34 + 1.36 * \sqrt[3]{\gamma_{st}} \qquad (29)$$

Then, with the use of machine learning, it was possible to obtain the equation that involved all the variables already defined as having a great influence on the buckling coefficient: aspect ratio, thickness ratio and haunch inclination. Also, the variable "sh" was added to define the relative position of the stiffener with respect to the height h_1 ($sh = h_{st1}/h_1$). If the value of this variable is 0.5, it is because the position of the stiffener is half height at half height, if it is different than 0.5, it is an inclined stiffener. The equation was then obtained:

$$k = k_H + 189 * sh + 159 * tan(\phi) + 17 * \left(\frac{t_f}{t_w}\right) + 3 * \left(\frac{a}{h_0}\right)^2 - 80 - 18 * \left(\frac{a}{h_0}\right) - 23 \qquad (30)$$
$$* \left(\frac{t_f}{t_w}\right) * sh - 184 * tan(\phi) * sh$$

57

6.1. Statistical evaluation

Figure 6-5 and Figure 6-6 show the correlation between the computed buckling coefficient k_s and those obtained with Eqs. (28) and (30), respectively.

It was found that for Eq. (28) there is a coefficient of determination R^2 of 0.97, which measures how a regression model fits the real data, and a relative variability of 5%, which indicates the variation with respect to the mean value of the relationship between the calculated k_s and the actual k_s. It is then found that the model found is very precise and does not have high dispersion, as can be seen in Figure 6-5.
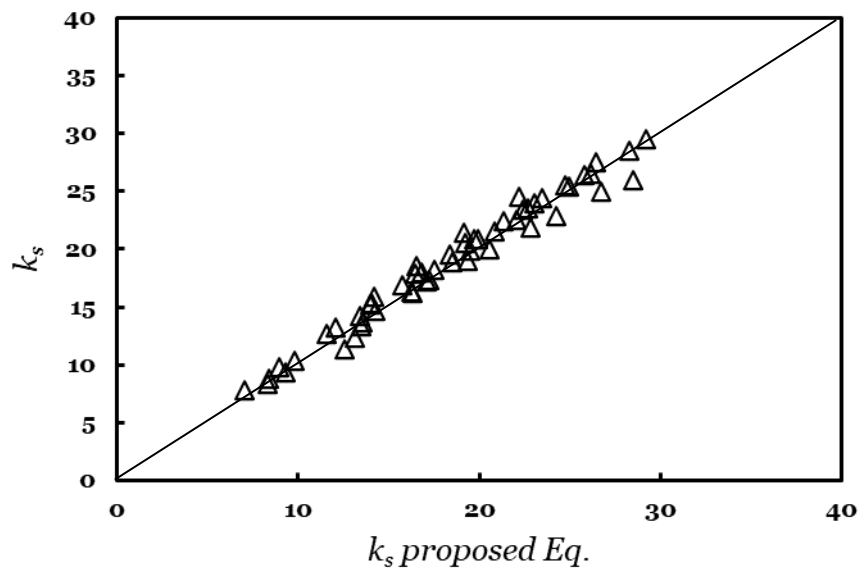
Figure 6-5. Correlation between numerical results and proposed formula for unstiffened case. Total cases = 54.

Also, it was found that for Eq. (30) there is a coefficient of determination R^2 of 0.94, which measures how a regression model fits the real data, and a relative variability of 6%, which indicates the variation with respect to the mean value of the relationship between the calculated k_s and the actual k_s. It is then found that the model found is very precise and does not have high dispersion, as can be seen in Figure 6-6.

It is important to clarify that these equations work very well in the range of parameters used to obtain them and that care must be taken when using them in another context.
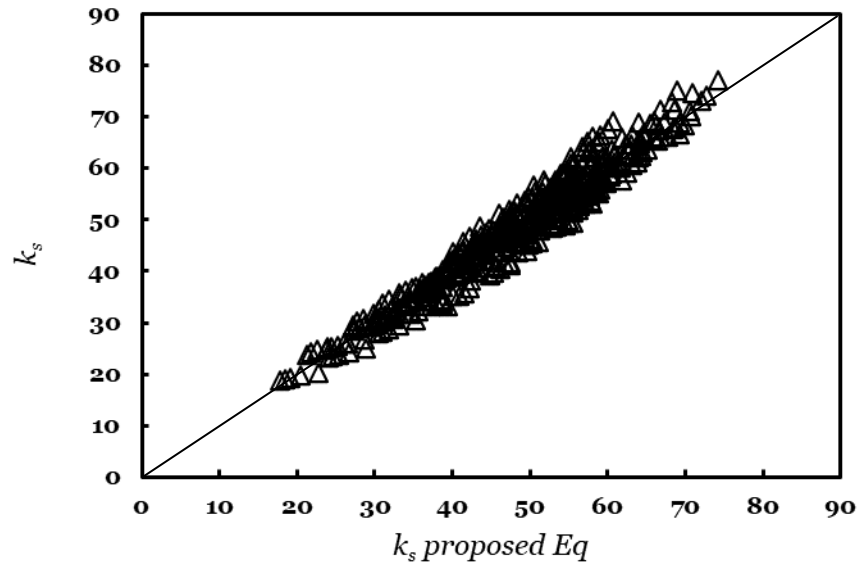
Figure 6-6. Correlation between numerical results and proposed formula for stiffened case. Total cases = 428.

7. Conclusions

In this thesis, the critical buckling response of longitudinally stiffened-haunched steel plate girders subjected to shear loading was investigated through finite element analysis. An extensive parametric study was performed, varying the panel aspect ratio, the flange-to-thickness ratio, the stiffener rigidity and location (mid-height, horizontal and inclined), along with different stiffener height positions. From the results the following conclusions are drawn:

- The use of longitudinal stiffeners increases the critical buckling coefficient k_s, and hence the critical stresses, of haunched girders subjected to shear loading.
- Regarding the flexural rigidity of the stiffener, within the range of parameters evaluated herein there is a diminished influence for $\gamma_s \geq 20$. Beyond this limit, buckling of the web panel is divided into two subpanels, and the whole girder attains a greater buckling load.
- The optimal position of a singular longitudinal stiffener is at half of one height, and it can be: to the other mid height or inclined with a relation of h_{st1}/h_1 greater than 0.5.
- The variables: aspect ratio, thickness ratio and haunch inclination have a very high influence on the buckling coefficient k_s. However, the slenderness ratio variable exerts a diminishing influence on this value. Nevertheless, including the web slenderness ratio is necessary for analyzing the ultimate strength behavior of longitudinally stiffened girders.
- Buckling coefficients calculated with the proposed formulas showed a very high correlation with the values computed numerically. This is very important to improve design codes and to review on new investigations.

7.1. Further research proposals

Below is a list of topics that can be investigated in future publications and thesis:

- Investigate the impact of using advanced materials (e.g., high-strength steel, composite materials) on the buckling response of longitudinally stiffened girders. This could involve comparing traditional steel girders with those made from newer, lighter, or more resilient materials to assess potential improvements in performance and efficiency.
- Conduct studies under more varied and realistic loading conditions, including dynamic loads, such as those caused by wind or seismic activity, to better

understand the performance of stiffened girders in real-world scenarios. The start can be adding loads such as shear-bending interaction and axial load.

- Examine the long-term performance and fatigue life of longitudinally stiffened-haunched steel plate girders, particularly focusing on the effects of cyclic loading over extended periods.

- Apply optimization techniques to the design of longitudinally stiffened girders, seeking the best possible configuration of stiffeners (including their number, positioning, and dimensions) for various loading scenarios.

- Perform comparative studies between longitudinally stiffened-haunched girders and alternative girder designs or structural systems, evaluating their performance, cost-effectiveness, and applicability in different architectural contexts.

- Explore the development of more sophisticated numerical models and simulation techniques, including non-linear analysis and the incorporation of material imperfections, to achieve more accurate predictions of buckling behavior.

- Study the influence of environmental conditions, such as temperature variations and corrosion, on the critical buckling response of steel girders.

- Conduct an in-depth investigation into the ultimate load-carrying capacity of longitudinally stiffened-haunched steel plate girders under various types of loading, including shear, bending, and combined loading scenarios. This study would also analyze the safety margins inherent in current design practices by comparing theoretical, numerical, and experimental ultimate loads.

8. References

[1] I. Estrada and E. Mirambell, "Abolladura por cortante en vigas armadas rigidizadas longitudinalmente," in *Enginyeria de Camins*, Barcelona, Escola Tècnica Superior d'Enginyeria de Camins, Canals i Ports de Barcelona, 2007. [In Spanish].

[2] D. Olds, "Two bridge projects show what's possible with a long-span I-girder scheme.," *AISC,* 2014.

[3] A. Bedynek, E. Real and E. Mirambell, "Tapered plate girders under shear: Tests and numerical research," *Engineering Structures,* p. 9, 2013.

[4] O. A. Sediek, S. S. Safar and M. M. Hassan, "Numerical investigation on shear strength of tapered perfect end web panels," *Structures,* pp. 354-368, 2020.

[5] S. P. Timoshenko and J. M. Gere, Theory of Elastic Stability, McGraw Hill, 1963.

[6] R. V. Southwell and S. W. Skan, "On the stability under shearing forces of a flat elastic strip," *Proceedings Royal Society,* p. 105, 1924.

[7] E. Seydel, "On the buckling of rectangular isotropic or orthogonal-isotropic plates by tangential stresses," *Ing. Arch.,* vol. 4, p. 169, 1933.

[8] M. Stein and J. Neff, "Buckling stresses of simply supported rectangular flat plates in shear," *Technical Note. NACA, Langley Field VA.,* no. 1222, 1947.

[9] F. Bleich, Buckling Strength of Metal Structures, New York: McGraw-Hill Book Co, 1952.

[10] S. C. Lee, J. S. Davidson and C. H. Yoo, "Shear buckling coefficients of plate girder web panels," *Computers & Structures,* pp. 789-795, 1996.

[11] E. Mirambell and A. V. Zárate, "Web buckling of tapered plate girders," *Proceedings of the Institution of Civil Engineers: Structures and Buildings,* pp. 51-60, 2000.

[12] A. Bedynek, E. Real and E. Mirambell, "Shear buckling coefficient: proposal for tapered steel plates," *Institution of Civil Engineers,* vol. 167, pp. 243-252, 2013.

[13] M. H. Serror, B. H. Abdelbaset and H. S. Sayed, "Shear strength of tapered end web panels," *Journal of Constructional Steel Research,* pp. 513-525, 2017.

[14] M. M. Ibrahim, I. M. El Aghoury and S. A.-B. Ibrahim, "Finite element investigation on plate buckling coefficients of tapered steel members web plates," *Structures,* 2020.

[15] The European Union, EN 1993-1-5 Eurocode 3, 2006.

[16] Cook and K. Rocky, *Aeronaut Quart,* vol. 13, no. 1, p. 41, 1962.

[17] T. Höglund, "Shear Buckling Resistance of Steel and Aluminium Plate Girders," *Thin-Walled Structures,* pp. 13-30, 1997.

[18] I. Estrada, E. Real and E. Mirambell, "Shear resistance in stainless steel plate girders with transverse and longitudinal stiffening," *Journal of Constructional Steel Research,* pp. 1239-1254, 2008.

[19] J. O. Ferreira, H. Carvalho, B. M. Silva, A. L. Reis, D. A. Barbosa, R. B. Caldas and J. P. Martins, "Linear buckling behavior of longitudinally singly- and multi-stiffened steel plates under normal and shear stresses," *Structures,* pp. 1209-1223, 2023.

[20] M. M. Alinia, "A study into optimization of stiffeners in plates subjected to shear loading," *Thin-Walled Structures,* no. 43, pp. 845-860, 2005.

[21] *Ansys 2024 R1*. [Performance]. ANSYS, Inc, 2024.

[22] A. R. de Faria, "Prebuckling Enhancement of Beams and Plates under Uncertain Loadings and Arbitrary Initial Imperfections," *Instituto Tecnológico de Aeronáutica – ITA,* vol. XXIX, no. 4, 2007.

[23] American Association of State Highway and Transportation, AASHTO LRFD Bridge Design Specifications., Washington, D.C., 2008.

[24] S. C. Lee and C. H. Yoo, "Strength of plate girder web panels under pure shear.," *Journal of Structural Engineering,* no. 124, pp. 184-194, 1998.

[25] E. Maiorana, C. Pellegrino and C. Modena, "Influence of longitudinal stiffeners on elastic stability of girders web," *Journal of Constructional Steel Research,* pp. 51-64, 2011.

[26] A. Bedynek, Structural behaviour of tapered steel plate girders subjected to shear. Doctoral Thesis., Barcelona: Universitat Politècnica de Catalunya, 2014.

[27] P. Rico, M. Echeverri and C. Graciano, "Shear buckling coefficients for longitudinally stiffened-haunched steel plate girders.," *Proceedings of the Annual Stability Conference Structural Stability Research Council Charlotte, North Carolina.,* 2023.

[28] I. DataRobot, Writer, *Eureqa Models.* [Performance]. DataRobot, Inc., 2024.

[29] B. H. AbdelAleem, M. K. Ismail, M. Haggag and El-Dakhakhni, "Interpretable soft computing predictions of elastic shear buckling in tapered steel plate girders.," *Thin-Walled Structures,* p. 17, 2022.

9. Appendix A: Numerical results.

The modeled data values for the girders with optimal position are presented:

h_0	b_{st0}	h_{st0}	a	b_f	h_1	h_{st1}	t_w	t_f	t_{st}	Load Multiplier
1000	62	500	1000	235	1176	588	6	12	4	1014253
1000	72	500	2000	271	1353	676	7	14	5	987654
1000	81	500	3000	306	1529	764	8	15	5	995672
1000	47	500	1000	235	1176	588	4	12	3	335778
1000	54	500	2000	271	1353	676	5	14	4	360215
1000	61	500	3000	306	1529	764	5	15	4	389466
1000	38	500	1000	235	1176	588	3	12	3	149678
1000	44	500	2000	271	1353	676	3	14	3	163940
1000	49	500	3000	306	1529	764	4	15	3	193219
1000	76	500	1000	235	1176	588	6	12	5	1051920
1000	87	500	2000	271	1353	676	7	14	6	1007706
1000	99	500	3000	306	1529	764	8	15	7	1009394
1000	57	500	1000	235	1176	588	4	12	4	348856
1000	65	500	2000	271	1353	676	5	14	4	371783
1000	74	500	3000	306	1529	764	5	15	5	395034
1000	46	500	1000	235	1176	588	3	12	3	155516
1000	53	500	2000	271	1353	676	3	14	4	175857
1000	60	500	3000	306	1529	764	4	15	4	196515
1000	93	500	1000	235	1176	588	6	12	6	1079224
1000	107	500	2000	271	1353	676	7	14	7	1023805
1000	121	500	3000	306	1529	764	8	15	8	1022270
1000	70	500	1000	235	1176	588	4	12	5	358102
1000	80	500	2000	271	1353	676	5	14	5	378343
1000	91	500	3000	306	1529	764	5	15	6	400227
1000	57	500	1000	235	1176	588	3	12	4	159653
1000	66	500	2000	271	1353	676	3	14	4	179482
1000	74	500	3000	306	1529	764	4	15	5	199367
1000	122	500	1000	235	1176	588	6	12	8	1115418
1000	140	500	2000	271	1353	676	7	14	9	1048048
1000	158	500	3000	306	1529	764	8	15	11	1043092
1000	92	500	1000	235	1176	588	4	12	6	370585
1000	106	500	2000	271	1353	676	5	14	7	388114
1000	119	500	3000	306	1529	764	5	15	8	408671
1000	75	500	1000	235	1176	588	3	12	5	165321
1000	86	500	2000	271	1353	676	3	14	6	184657
1000	98	500	3000	306	1529	764	4	15	7	203891
1000	170	500	1000	235	1176	588	6	12	11	1159476
1000	196	500	2000	271	1353	676	7	14	13	1079176
1000	221	500	3000	306	1529	764	8	15	15	1070411
1000	128	500	1000	235	1176	588	4	12	9	385610

1000	148	500	2000	271	1353	676	5	14	10	399915
1000	167	500	3000	306	1529	764	5	15	11	419047
1000	105	500	1000	235	1176	588	3	12	7	172070
1000	121	500	2000	271	1353	676	3	14	8	190606
1000	137	500	3000	306	1529	764	4	15	9	209187
1000	67	500	1000	254	1268	634	6	13	4	1338980
1000	81	500	2000	307	1536	768	8	15	5	1516252
1000	96	500	3000	361	1804	902	9	18	6	1707965
1000	50	500	1000	254	1268	634	4	13	3	445102
1000	61	500	2000	307	1536	768	5	15	4	557428
1000	72	500	3000	361	1804	902	6	18	5	668352
1000	41	500	1000	254	1268	634	3	13	3	198238
1000	50	500	2000	307	1536	768	4	15	3	258459
1000	58	500	3000	361	1804	902	5	18	4	334648
1000	82	500	1000	254	1268	634	6	13	5	1384557
1000	99	500	2000	307	1536	768	8	15	7	1544313
1000	117	500	3000	361	1804	902	9	18	8	1731127
1000	61	500	1000	254	1268	634	4	13	4	460546
1000	74	500	2000	307	1536	768	5	15	5	571172
1000	87	500	3000	361	1804	902	6	18	6	677570
1000	50	500	1000	254	1268	634	3	13	3	205019
1000	61	500	2000	307	1536	768	4	15	4	271183
1000	71	500	3000	361	1804	902	5	18	5	340010
1000	100	500	1000	254	1268	634	6	13	7	1419825
1000	121	500	2000	307	1536	768	8	15	8	1569656
1000	142	500	3000	361	1804	902	9	18	9	1754650
1000	75	500	1000	254	1268	634	4	13	5	472380
1000	91	500	2000	307	1536	768	5	15	6	581332
1000	107	500	3000	361	1804	902	6	18	7	686965
1000	61	500	1000	254	1268	634	3	13	4	210181
1000	74	500	2000	307	1536	768	4	15	5	276818
1000	87	500	3000	361	1804	902	5	18	6	345095
1000	131	500	1000	254	1268	634	6	13	9	1469358
1000	159	500	2000	307	1536	768	8	15	11	1610144
1000	187	500	3000	361	1804	902	9	18	12	1794359
1000	99	500	1000	254	1268	634	4	13	7	489211
1000	120	500	2000	307	1536	768	5	15	8	597307
1000	141	500	3000	361	1804	902	6	18	9	702598
1000	81	500	1000	254	1268	634	3	13	5	217766
1000	98	500	2000	307	1536	768	4	15	7	285224
1000	115	500	3000	361	1804	902	5	18	8	353371
1000	183	500	1000	254	1268	634	6	13	12	1532177
1000	222	500	2000	307	1536	768	8	15	15	1664644
1000	261	500	3000	361	1804	902	9	18	17	1849394
1000	138	500	1000	254	1268	634	4	13	9	510177

1000	168	500	2000	307	1536	768	5	15	11	617439
1000	197	500	3000	361	1804	902	6	18	13	722871
1000	113	500	1000	254	1268	634	3	13	8	227020
1000	137	500	2000	307	1536	768	4	15	9	295118
1000	161	500	3000	361	1804	902	5	18	11	363502
1000	72	500	1000	273	1364	682	7	14	5	1763944
1000	92	500	2000	346	1728	864	9	17	6	2260776
1000	111	500	3000	418	2092	1046	10	21	7	2767758
1000	54	500	1000	273	1364	682	5	14	4	588187
1000	69	500	2000	346	1728	864	6	17	5	839228
1000	83	500	3000	418	2092	1046	7	21	6	1089740
1000	44	500	1000	273	1364	682	3	14	3	262386
1000	56	500	2000	346	1728	864	4	17	4	394764
1000	68	500	3000	418	2092	1046	5	21	5	549443
1000	88	500	1000	273	1364	682	7	14	6	1819863
1000	112	500	2000	346	1728	864	9	17	7	2300224
1000	135	500	3000	418	2092	1046	10	21	9	2805496
1000	66	500	1000	273	1364	682	5	14	4	606779
1000	84	500	2000	346	1728	864	6	17	6	856915
1000	101	500	3000	418	2092	1046	7	21	7	1104485
1000	54	500	1000	273	1364	682	3	14	4	270471
1000	68	500	2000	346	1728	864	4	17	5	408691
1000	83	500	3000	418	2092	1046	5	21	6	557685
1000	108	500	1000	273	1364	682	7	14	7	1866717
1000	136	500	2000	346	1728	864	9	17	9	2339858
1000	165	500	3000	418	2092	1046	10	21	11	2847150
1000	81	500	1000	273	1364	682	5	14	5	622239
1000	102	500	2000	346	1728	864	6	17	7	872612
1000	124	500	3000	418	2092	1046	7	21	8	1120788
1000	66	500	1000	273	1364	682	3	14	4	277191
1000	84	500	2000	346	1728	864	4	17	6	417286
1000	101	500	3000	418	2092	1046	5	21	7	566406
1000	141	500	1000	273	1364	682	7	14	9	1935512
1000	179	500	2000	346	1728	864	9	17	12	2406249
1000	217	500	3000	418	2092	1046	10	21	14	2919911
1000	106	500	1000	273	1364	682	5	14	7	645425
1000	135	500	2000	346	1728	864	6	17	9	898358
1000	163	500	3000	418	2092	1046	7	21	11	1148803
1000	87	500	1000	273	1364	682	3	14	6	287518
1000	110	500	2000	346	1728	864	4	17	7	430704
1000	134	500	3000	418	2092	1046	5	21	9	580956
1000	197	500	1000	273	1364	682	7	14	13	2026991
1000	250	500	2000	346	1728	864	9	17	17	2500560
1000	303	500	3000	418	2092	1046	10	21	20	3026000
1000	149	500	1000	273	1364	682	5	14	10	675384

1000	189	500	2000	346	1728	864	6	17	13	932301
1000	228	500	3000	418	2092	1046	7	21	15	1187121
1000	122	500	1000	273	1364	682	3	14	8	300566
1000	154	500	2000	346	1728	864	4	17	10	447004
1000	187	500	3000	418	2092	1046	5	21	12	599558
1000	78	500	1000	293	1466	733	7	15	5	2327758
1000	103	500	2000	387	1933	966	10	19	7	3307369
1000	127	500	3000	480	2399	1199	12	24	8	4319361
1000	58	500	1000	293	1466	733	5	15	4	779301
1000	77	500	2000	387	1933	966	6	19	5	1242400
1000	95	500	3000	480	2399	1199	8	24	6	1716893
1000	47	500	1000	293	1466	733	4	15	3	349684
1000	62	500	2000	387	1933	966	5	19	4	592244
1000	77	500	3000	480	2399	1199	6	24	5	872542
1000	95	500	1000	293	1466	733	7	15	6	2397424
1000	125	500	2000	387	1933	966	10	19	8	3363408
1000	155	500	3000	480	2399	1199	12	24	10	4380383
1000	71	500	1000	293	1466	733	5	15	5	802229
1000	94	500	2000	387	1933	966	6	19	6	1265727
1000	116	500	3000	480	2399	1199	8	24	8	1740239
1000	58	500	1000	293	1466	733	4	15	4	359634
1000	76	500	2000	387	1933	966	5	19	5	608301
1000	95	500	3000	480	2399	1199	6	24	6	884994
1000	116	500	1000	293	1466	733	7	15	8	2460529
1000	153	500	2000	387	1933	966	10	19	10	3425778
1000	189	500	3000	480	2399	1199	12	24	13	4452647
1000	87	500	1000	293	1466	733	5	15	6	822912
1000	115	500	2000	387	1933	966	6	19	8	1289901
1000	142	500	3000	480	2399	1199	8	24	9	1768043
1000	71	500	1000	293	1466	733	4	15	5	368676
1000	94	500	2000	387	1933	966	5	19	6	621218
1000	116	500	3000	480	2399	1199	6	24	8	899544
1000	152	500	1000	293	1466	733	7	15	10	2558479
1000	200	500	2000	387	1933	966	10	19	13	3534341
1000	248	500	3000	480	2399	1199	12	24	17	4582879
1000	114	500	1000	293	1466	733	5	15	8	855469
1000	151	500	2000	387	1933	966	6	19	10	1331234
1000	187	500	3000	480	2399	1199	8	24	12	1817144
1000	94	500	1000	293	1466	733	4	15	6	383121
1000	123	500	2000	387	1933	966	5	19	8	642484
1000	153	500	3000	480	2399	1199	6	24	10	924546
1000	212	500	1000	293	1466	733	7	15	14	2693029
1000	279	500	2000	387	1933	966	10	19	19	3695703
1000	347	500	3000	480	2399	1199	12	24	23	4781052
1000	160	500	1000	293	1466	733	5	15	11	899172

1000	211	500	2000	387	1933	966	6	19	14	1388433
1000	262	500	3000	480	2399	1199	8	24	17	1888168
1000	131	500	1000	293	1466	733	4	15	9	401959
1000	173	500	2000	387	1933	966	5	19	12	669364
1000	214	500	3000	480	2399	1199	6	24	14	958294
1000	84	500	1000	315	1577	789	8	16	6	3107273
1000	114	500	2000	431	2155	1077	11	22	8	4793787
1000	145	500	3000	546	2732	1366	14	27	10	6605467
1000	63	500	1000	315	1577	789	5	16	4	1044789
1000	85	500	2000	431	2155	1077	7	22	6	1826893
1000	108	500	3000	546	2732	1366	9	27	7	2638733
1000	51	500	1000	315	1577	789	4	16	3	467740
1000	70	500	2000	431	2155	1077	5	22	5	886718
1000	88	500	3000	546	2732	1366	7	27	6	1352957
1000	102	500	1000	315	1577	789	8	16	7	3196747
1000	139	500	2000	431	2155	1077	11	22	9	4876072
1000	176	500	3000	546	2732	1366	14	27	12	6704956
1000	76	500	1000	315	1577	789	5	16	5	1073993
1000	104	500	2000	431	2155	1077	7	22	7	1858711
1000	132	500	3000	546	2732	1366	9	27	9	2675850
1000	62	500	1000	315	1577	789	4	16	4	480031
1000	85	500	2000	431	2155	1077	5	22	6	905400
1000	108	500	3000	546	2732	1366	7	27	7	1372184
1000	125	500	1000	315	1577	789	8	16	8	3284268
1000	170	500	2000	431	2155	1077	11	22	11	4975172
1000	216	500	3000	546	2732	1366	14	27	14	6829857
1000	94	500	1000	315	1577	789	5	16	6	1102406
1000	128	500	2000	431	2155	1077	7	22	9	1896512
1000	162	500	3000	546	2732	1366	9	27	11	2722862
1000	76	500	1000	315	1577	789	4	16	5	492386
1000	104	500	2000	431	2155	1077	5	22	7	925300
1000	132	500	3000	546	2732	1366	7	27	9	1396262
1000	163	500	1000	315	1577	789	8	16	11	3426836
1000	223	500	2000	431	2155	1077	11	22	15	5153395
1000	283	500	3000	546	2732	1366	14	27	19	7060004
1000	123	500	1000	315	1577	789	5	16	8	1149977
1000	168	500	2000	431	2155	1077	7	22	11	1963043
1000	213	500	3000	546	2732	1366	9	27	14	2808047
1000	101	500	1000	315	1577	789	4	16	7	513220
1000	138	500	2000	431	2155	1077	5	22	9	959408
1000	175	500	3000	546	2732	1366	7	27	12	1438748
1000	228	500	1000	315	1577	789	8	16	15	3629272
1000	312	500	2000	431	2155	1077	11	22	21	5429321
1000	395	500	3000	546	2732	1366	14	27	26	7423697
1000	172	500	1000	315	1577	789	5	16	11	1215715

1000	235	500	2000	431	2155	1077	7	22	16	2060281
1000	298	500	3000	546	2732	1366	9	27	20	2937218
1000	141	500	1000	315	1577	789	4	16	9	541242
1000	192	500	2000	431	2155	1077	5	22	13	1004636
1000	244	500	3000	546	2732	1366	7	27	16	1499431
1000	62	500	1000	235	1176	676	6	12	4	1206025
1000	72	500	2000	271	1353	853	7	14	5	1336479
1000	81	500	3000	306	1529	1029	8	15	5	1578321
1000	47	500	1000	235	1176	676	4	12	3	396160
1000	54	500	2000	271	1353	853	5	14	4	422969
1000	61	500	3000	306	1529	1029	5	15	4	529030
1000	38	500	1000	235	1176	676	3	12	3	174892
1000	44	500	2000	271	1353	853	3	14	3	182180
1000	49	500	3000	306	1529	1029	4	15	3	232896
1000	76	500	1000	235	1176	676	6	12	5	1258940
1000	87	500	2000	271	1353	853	7	14	6	1413015
1000	99	500	3000	306	1529	1029	8	15	7	1631440
1000	57	500	1000	235	1176	676	4	12	4	413046
1000	65	500	2000	271	1353	853	5	14	4	500112
1000	74	500	3000	306	1529	1029	5	15	5	637107
1000	46	500	1000	235	1176	676	3	12	3	181426
1000	53	500	2000	271	1353	853	3	14	4	212649
1000	60	500	3000	306	1529	1029	4	15	4	275416
1000	93	500	1000	235	1176	676	6	12	6	1298304
1000	107	500	2000	271	1353	853	7	14	7	1447269
1000	121	500	3000	306	1529	1029	8	15	8	1673961
1000	70	500	1000	235	1176	676	4	12	5	425054
1000	80	500	2000	271	1353	853	5	14	5	534284
1000	91	500	3000	306	1529	1029	5	15	6	661359
1000	57	500	1000	235	1176	676	3	12	4	186118
1000	66	500	2000	271	1353	853	3	14	4	230126
1000	74	500	3000	306	1529	1029	4	15	5	308628
1000	122	500	1000	235	1176	676	6	12	8	1359016
1000	140	500	2000	271	1353	853	7	14	9	1511420
1000	158	500	3000	306	1529	1029	8	15	11	1757615
1000	92	500	1000	235	1176	676	4	12	6	445041
1000	106	500	2000	271	1353	853	5	14	7	561091
1000	119	500	3000	306	1529	1029	5	15	8	691730
1000	75	500	1000	235	1176	676	3	12	5	194554
1000	86	500	2000	271	1353	853	3	14	6	245294
1000	98	500	3000	306	1529	1029	4	15	7	328778
1000	170	500	1000	235	1176	676	6	12	11	1445036
1000	196	500	2000	271	1353	853	7	14	13	1612793
1000	221	500	3000	306	1529	1029	8	15	15	1895146
1000	128	500	1000	235	1176	676	4	12	9	474461

1000	148	500	2000	271	1353	853	5	14	10	596404
1000	167	500	3000	306	1529	1029	5	15	11	736830
1000	105	500	1000	235	1176	676	3	12	7	206436
1000	121	500	2000	271	1353	853	3	14	8	260758
1000	137	500	3000	306	1529	1029	4	15	9	349806
1000	67	500	1000	254	1268	768	6	13	4	1732226
1000	81	500	2000	307	1536	1036	8	15	5	2125111
1000	96	500	3000	361	1804	1304	9	18	6	2806789
1000	50	500	1000	254	1268	768	4	13	3	555460
1000	61	500	2000	307	1536	1036	5	15	4	648357
1000	72	500	3000	361	1804	1304	6	18	5	891235
1000	41	500	1000	254	1268	768	3	13	3	233528
1000	50	500	2000	307	1536	1036	4	15	3	275016
1000	58	500	3000	361	1804	1304	5	18	4	382701
1000	82	500	1000	254	1268	768	6	13	5	1796603
1000	99	500	2000	307	1536	1036	8	15	7	2430765
1000	117	500	3000	361	1804	1304	9	18	8	3357436
1000	61	500	1000	254	1268	768	4	13	4	567993
1000	74	500	2000	307	1536	1036	5	15	5	724295
1000	87	500	3000	361	1804	1304	6	18	6	1013683
1000	50	500	1000	254	1268	768	3	13	3	239354
1000	61	500	2000	307	1536	1036	4	15	4	302453
1000	71	500	3000	361	1804	1304	5	18	5	423807
1000	100	500	1000	254	1268	768	6	13	7	1848863
1000	121	500	2000	307	1536	1036	8	15	8	2574736
1000	142	500	3000	361	1804	1304	9	18	9	3572318
1000	75	500	1000	254	1268	768	4	13	5	580354
1000	91	500	2000	307	1536	1036	5	15	6	767753
1000	107	500	3000	361	1804	1304	6	18	7	1089905
1000	61	500	1000	254	1268	768	3	13	4	244216
1000	74	500	2000	307	1536	1036	4	15	5	318283
1000	87	500	3000	361	1804	1304	5	18	6	448660
1000	131	500	1000	254	1268	768	6	13	9	1943204
1000	159	500	2000	307	1536	1036	8	15	11	2735211
1000	187	500	3000	361	1804	1304	9	18	12	3811451
1000	99	500	1000	254	1268	768	4	13	7	602402
1000	120	500	2000	307	1536	1036	5	15	8	810337
1000	141	500	3000	361	1804	1304	6	18	9	1157320
1000	81	500	1000	254	1268	768	3	13	5	252074
1000	98	500	2000	307	1536	1036	4	15	7	334096
1000	115	500	3000	361	1804	1304	5	18	8	472821
1000	183	500	1000	254	1268	768	6	13	12	2094908
1000	222	500	2000	307	1536	1036	8	15	15	2986681
1000	261	500	3000	361	1804	1304	9	18	17	4218602
1000	138	500	1000	254	1268	768	4	13	9	628105

1000	168	500	2000	307	1536	1036	5	15	11	856191
1000	197	500	3000	361	1804	1304	6	18	13	1236000
1000	113	500	1000	254	1268	768	3	13	8	260865
1000	137	500	2000	307	1536	1036	4	15	9	350627
1000	161	500	3000	361	1804	1304	5	18	11	500635
1000	72	500	1000	273	1364	864	7	14	5	2353344
1000	92	500	2000	346	1728	1228	9	17	6	3053021
1000	111	500	3000	418	2092	1592	10	21	7	4354910
1000	54	500	1000	273	1364	864	5	14	4	701150
1000	69	500	2000	346	1728	1228	6	17	5	912611
1000	83	500	3000	418	2092	1592	7	21	6	1330770
1000	44	500	1000	273	1364	864	3	14	3	294382
1000	56	500	2000	346	1728	1228	4	17	4	384468
1000	68	500	3000	418	2092	1592	5	21	5	564170
1000	88	500	1000	273	1364	864	7	14	6	2415173
1000	112	500	2000	346	1728	1228	9	17	7	3343599
1000	135	500	3000	418	2092	1592	10	21	9	4897169
1000	66	500	1000	273	1364	864	5	14	4	719199
1000	84	500	2000	346	1728	1228	6	17	6	981108
1000	101	500	3000	418	2092	1592	7	21	7	1443903
1000	54	500	1000	273	1364	864	3	14	4	301422
1000	68	500	2000	346	1728	1228	4	17	5	409535
1000	83	500	3000	418	2092	1592	5	21	6	603384
1000	108	500	1000	273	1364	864	7	14	7	2469857
1000	136	500	2000	346	1728	1228	9	17	9	3522601
1000	165	500	3000	418	2092	1592	10	21	11	5239865
1000	81	500	1000	273	1364	864	5	14	5	734148
1000	102	500	2000	346	1728	1228	6	17	7	1025223
1000	124	500	3000	418	2092	1592	7	21	8	1520617
1000	66	500	1000	273	1364	864	3	14	4	307260
1000	84	500	2000	346	1728	1228	4	17	6	426062
1000	101	500	3000	418	2092	1592	5	21	7	630753
1000	141	500	1000	273	1364	864	7	14	9	2562136
1000	179	500	2000	346	1728	1228	9	17	12	3726272
1000	217	500	3000	418	2092	1592	10	21	14	5611856
1000	106	500	1000	273	1364	864	5	14	7	756567
1000	135	500	2000	346	1728	1228	6	17	9	1075757
1000	163	500	3000	418	2092	1592	7	21	11	1609355
1000	87	500	1000	273	1364	864	3	14	6	315906
1000	110	500	2000	346	1728	1228	4	17	7	445052
1000	134	500	3000	418	2092	1592	5	21	9	662804
1000	197	500	1000	273	1364	864	7	14	13	2676369
1000	250	500	2000	346	1728	1228	9	17	17	3982847
1000	303	500	3000	418	2092	1592	10	21	20	6147200
1000	149	500	1000	273	1364	864	5	14	10	784299

1000	189	500	2000	346	1728	1228	6	17	13	1135898
1000	228	500	3000	418	2092	1592	7	21	15	1725971
1000	122	500	1000	273	1364	864	3	14	8	326375
1000	154	500	2000	346	1728	1228	4	17	10	466732
1000	187	500	3000	418	2092	1592	5	21	12	702898
1000	78	500	1000	293	1466	966	7	15	5	2932878
1000	103	500	2000	387	1933	1433	10	19	7	4135445
1000	127	500	3000	480	2399	1899	12	24	8	6153964
1000	58	500	1000	293	1466	966	5	15	4	875989
1000	77	500	2000	387	1933	1433	6	19	5	1234213
1000	95	500	3000	480	2399	1899	8	24	6	1881498
1000	47	500	1000	293	1466	966	4	15	3	371046
1000	62	500	2000	387	1933	1433	5	19	4	521554
1000	77	500	3000	480	2399	1899	6	24	5	801078
1000	95	500	1000	293	1466	966	7	15	6	3018449
1000	125	500	2000	387	1933	1433	10	19	8	4420161
1000	155	500	3000	480	2399	1899	12	24	10	6688633
1000	71	500	1000	293	1466	966	5	15	5	897677
1000	94	500	2000	387	1933	1433	6	19	6	1303284
1000	116	500	3000	480	2399	1899	8	24	8	2002504
1000	58	500	1000	293	1466	966	4	15	4	379381
1000	76	500	2000	387	1933	1433	5	19	5	547439
1000	95	500	3000	480	2399	1899	6	24	6	844515
1000	116	500	1000	293	1466	966	7	15	8	3090900
1000	153	500	2000	387	1933	1433	10	19	10	4624542
1000	189	500	3000	480	2399	1899	12	24	13	7084695
1000	87	500	1000	293	1466	966	5	15	6	916601
1000	115	500	2000	387	1933	1433	6	19	8	1354223
1000	142	500	3000	480	2399	1899	8	24	9	2096004
1000	71	500	1000	293	1466	966	4	15	5	386735
1000	94	500	2000	387	1933	1433	5	19	6	566651
1000	116	500	3000	480	2399	1899	6	24	8	878485
1000	152	500	1000	293	1466	966	7	15	10	3200599
1000	200	500	2000	387	1933	1433	10	19	13	4891519
1000	248	500	3000	480	2399	1899	12	24	17	7622745
1000	114	500	1000	293	1466	966	5	15	8	945122
1000	151	500	2000	387	1933	1433	6	19	10	1420072
1000	187	500	3000	480	2399	1899	8	24	12	2220244
1000	94	500	1000	293	1466	966	4	15	6	397801
1000	123	500	2000	387	1933	1433	5	19	8	591171
1000	153	500	3000	480	2399	1899	6	24	10	922722
1000	212	500	1000	293	1466	966	7	15	14	3348008
1000	279	500	2000	387	1933	1433	10	19	19	5260286
1000	347	500	3000	480	2399	1899	12	24	23	8465284
1000	160	500	1000	293	1466	966	5	15	11	983403

1000	211	500	2000	387	1933	1433	6	19	14	1505596
1000	262	500	3000	480	2399	1899	8	24	17	2398004
1000	131	500	1000	293	1466	966	4	15	9	412313
1000	173	500	2000	387	1933	1433	5	19	12	621510
1000	214	500	3000	480	2399	1899	6	24	14	982085
1000	84	500	1000	315	1577	1077	8	16	6	3651741
1000	114	500	2000	431	2155	1655	11	22	8	5478754
1000	145	500	3000	546	2732	2232	14	27	10	8379940
1000	63	500	1000	315	1577	1077	5	16	4	1096224
1000	85	500	2000	431	2155	1655	7	22	6	1650678
1000	108	500	3000	546	2732	2232	9	27	7	2604736
1000	51	500	1000	315	1577	1077	4	16	3	464757
1000	70	500	2000	431	2155	1655	5	22	5	704842
1000	88	500	3000	546	2732	2232	7	27	6	1121075
1000	102	500	1000	315	1577	1077	8	16	7	3758707
1000	139	500	2000	431	2155	1655	11	22	9	5792976
1000	176	500	3000	546	2732	2232	14	27	12	8988441
1000	76	500	1000	315	1577	1077	5	16	5	1122920
1000	104	500	2000	431	2155	1655	7	22	7	1727785
1000	132	500	3000	546	2732	2232	9	27	9	2748491
1000	62	500	1000	315	1577	1077	4	16	4	474698
1000	85	500	2000	431	2155	1655	5	22	6	734159
1000	108	500	3000	546	2732	2232	7	27	7	1173834
1000	125	500	1000	315	1577	1077	8	16	8	3856178
1000	170	500	2000	431	2155	1655	11	22	11	6049036
1000	216	500	3000	546	2732	2232	14	27	14	9508310
1000	94	500	1000	315	1577	1077	5	16	6	1147755
1000	128	500	2000	431	2155	1655	7	22	9	1791550
1000	162	500	3000	546	2732	2232	9	27	11	2870795
1000	76	500	1000	315	1577	1077	4	16	5	484282
1000	104	500	2000	431	2155	1655	5	22	7	758256
1000	132	500	3000	546	2732	2232	7	27	9	1218230
1000	163	500	1000	315	1577	1077	8	16	11	4008110
1000	223	500	2000	431	2155	1655	11	22	15	6419700
1000	283	500	3000	546	2732	2232	14	27	19	10306188
1000	123	500	1000	315	1577	1077	5	16	8	1187297
1000	168	500	2000	431	2155	1655	7	22	11	1880996
1000	213	500	3000	546	2732	2232	9	27	14	3048401
1000	101	500	1000	315	1577	1077	4	16	7	499390
1000	138	500	2000	431	2155	1655	5	22	9	791366
1000	175	500	3000	546	2732	2232	7	27	12	1280383
1000	228	500	1000	315	1577	1077	8	16	15	4225563
1000	312	500	2000	431	2155	1655	11	22	21	6976052
1000	395	500	3000	546	2732	2232	14	27	26	11635884
1000	172	500	1000	315	1577	1077	5	16	11	1243367

1000	235	500	2000	431	2155	1655	7	22	16	2006920
1000	298	500	3000	546	2732	2232	9	27	20	3318576
1000	141	500	1000	315	1577	1077	4	16	9	520439
1000	192	500	2000	431	2155	1655	5	22	13	835517
1000	244	500	3000	546	2732	2232	7	27	16	1368744

10. Appendix B: Conference paper

Shear buckling coefficients for longitudinally stiffened-haunched steel plate girders

Pablo Rico[1], Mariana Echeverri[2], Carlos Graciano[3]

Abstract

In this paper, the critical buckling behavior of haunched steel plate girders subjected to shear loading is investigated in depth. The study is conducted through linear buckling analysis using the finite element method. First, the results are validated with previous results for simply supported rectangular and nonrectangular web panels. Thereafter, an extensive parametric study is conducted to investigate the influence of various geometric parameters including the inclination angle, the panel aspect ratio, the size of the flanges and the presence of longitudinal stiffeners on the buckling coefficients. Finally, the results are employed to develop expressions for the shear buckling coefficients for longitudinally stiffened-haunched steel plate girders taking into account the forementioned parameters.

1. Introduction

In modern construction, sustainability has become an important factor in structural design. In sustainable design, the use of traditional materials is optimized or new materials are employed. In this sense, girder with haunches, also called tapered girders or nonrectangular panels, are increasingly employed particularly in the design of steel bridges curved in elevation. In this case, the girder depth is reduced from intermediate supports (maximum depth) to mid span (minimum depth). Over the last decades, tapered girders have been the focus of several research projects, nevertheless this paper is aimed at analyzing tapered plate girder subject to shear.

Usually, two types of analysis are performed to investigate the shear response of tapered steel girders, ultimate strength analysis and linear buckling analysis. The shear strength of unstiffened tapered girder webs has been investigated experimentally and numerically (Mirambell and Zarate 2000, Zarate and Mirambell 2004, Real et al. 2010, Bedynek et al. 2013, Bedynek 2014, Bedynek et al. 2017, Ibrahin et al. 2020, Sediek et al. 2020). The effect of longitudinal stiffening on the shear strength of tapered plate girders was also investigated (Bedynek et al. 2013, Bedynek 2014). Compared to flat web plates, corrugated plates offer an enhanced out-of-plane stiffness that can increase the shear strength of tapered girders (Hassanein and Kharoob 2014, Hassanein and Kharoob 2015, Zevallos et al.

---

[1] Graduate Research Assistant, Universidad Nacional de Colombia, <pricog@unal.edu.co>
[2] Undergraduate student, Universidad Nacional de Colombia, <mecheverrilo@unal.edu.co>
[3] Full Professor, Universidad Nacional de Colombia, <cagracianog@unal.edu.co>

2016). Linear buckling analyses of unstiffened tapered web girder have also been performed (Bedynek et al. 2013, Bedynek et al. 2014, Ibrahim et al. 2020; AbdelAleem et al. 2022). In these linear analyses, the influence of the girder flanges was disregarded.

Recently, the strength of longitudinally stiffened tapered girder web panels subjected to combined bending and shear was investigated experimentally and numerically (Poroustad and Kuhlmann 2018, Poroustad and Kuhlmann 2018, Kuhlmann et al. 2020, Poroustad and Kuhlmann 2021). In these studies, the tapered girders had one horizontal flange and an inclined one, and the longitudinal stiffener was placed either parallel to the upper or lower flange. Furthermore, in the loading protocol the inclined flange was always under compression.

As seen above, there is a still a need to investigate the critical buckling response of longitudinally stiffened-haunched girders subject to shear. Therefore, this paper aims at investigating the linear buckling response of this type of girders. The study in conducted numerically through linear buckling analysis using the finite element method. Firstly, a numerical model is built for simply supported rectangular panel subject to shear loading. Once the model is validated, the geometry is extended to longitudinally stiffened-haunched girders. After that, a parametric analysis is performed to investigate the influence of various geometric variables including the inclination angle, the panel aspect ratio, the size of the flanges and the presence of longitudinal stiffeners on the buckling coefficients. In the end, the results from the parametric study are employed to develop expressions for the shear buckling coefficients for longitudinally stiffened-haunched steel plate girders.

2. Numerical modeling

Fig. 1 shows the nomenclature used herein for longitudinally stiffened-haunched plate girders. A finite element model is developed using the software ANSYS (ANSYS 2022). Shell 181 elements, with four nodes and six degrees of freedom on each node are employed to model the girder components (flanges, web and stiffener). A unit load is applied downward in the web at the lower height end, as shown in Fig. 2. Through eigenvalue buckling analysis, critical buckling stresses τ_{cr} are computed, and according to the theory of plates stability, buckling coefficients are obtained. The critical buckling shear stress for a simply supported rectangular plate is expressed as

$$\tau_{cr} = k_s \frac{\pi^2 E}{12(1-\nu^2)} \left(\frac{t_w}{h}\right)^2 \tag{1}$$

where k_s is the shear buckling coefficient, E is the modulus of elasticity, ν is the Poisson's ratio, h is the web depth, and t_w is web thickness.

2.1 Geometry and parameters

Table 1 presents the variables and their range for the parametric study. This geometry is intended to recreate the behavior of haunched girders near the supports of bridges, in which the inclined flange is under compression and the tension field is developed in the short diagonal. Through the analysis, the longitudinal stiffener is always located from mid height of the lower end ($h_0/2$), and varies its inclination: horizontal, parallel to the inclined flange, and from mid-height ($h_1/2$) to mid-height ($h_0/2$).
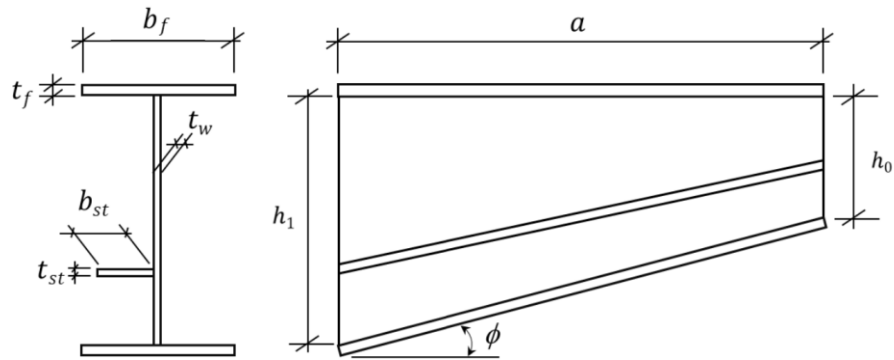
Figure 1: Geometry of longitudinally stiffened-haunched plate girder (Nomenclature)

Table 1: Parameters

Parameters	
Dimension	Value
h_o [mm]	1000
b_f	$h_1/6$
ϕ [°]	0, 10, 15, 20, 30
a/h_o	1, 2, 3
h_1/t_w	150, 200, 300
t_f/t_w	1, 2, 3
γ_s	0, 10, 20, 60, 150
Stiffener position	Horizontal, Inclined, Mid-Height
E [MPa]	210000
v	0.3
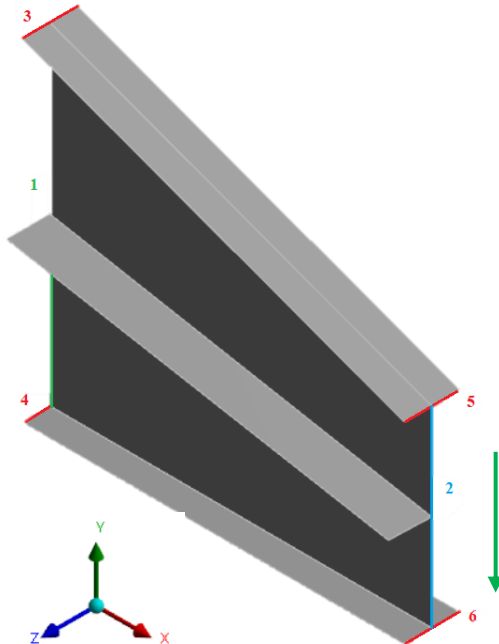
Figure 2: Boundary conditions.

The boundary conditions are shown in Fig. 2 and Table 2. The load is applied downward at the web in the lower end. With this configuration, the tension field is developed in the short diagonal and the inclined flange is under compression.

Table 2: Boundary conditions

Location	Degree of freedom						
	U_x	U_y	U_z	R_x	R_y	R_z	Force
1	R	R	R	R	F	R	0
2	F	F	R	R	F	R	$-U_y$
3, 4, 5, 6	F	F	R	R	R	F	0

*F denotes free and R denotes restrained

2.2 Validation procedure

The following material properties were used throughout the study: E= 210000 MPa and v = 0.3. A mesh converge analysis was conducted in Fig. 3 for an unstiffened girder with small flanges, with the following dimensions $a/h_0 = 1$, $\phi = 15°$, $h_1/t_w = 150$, and $t_f/t_w = 1$. As seen in Fig. 4, the variation in the buckling coefficient is small when for element sizes of 40 mm, hence this element size is chosen for further analysis.
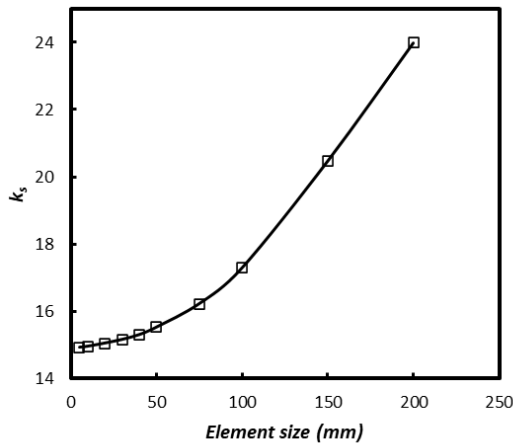
Figure 3. Mesh convergence analysis
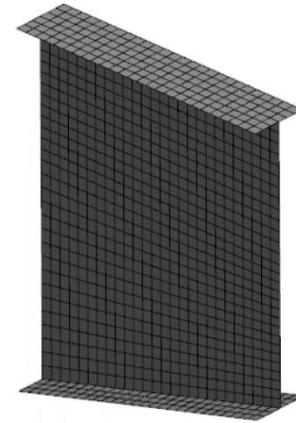
Figure 4. Final mesh

In the literature (Timoshenko and Gere 1936, Ziemian 2010), the shear buckling coefficient for a simply supported rectangular plate subjected to shear is

$$k_s = 5.34 + 4 \left(\frac{h}{a}\right)^2 \tag{2}$$

Also, for non-rectangular simply supported plates, (Bedynek, 2013) proposed four different equations depending on the geometry of the plate and loading direction. For a girder with the inclined flange under compression and the diagonal tension field developed in the short diagonal,

79

$$k_s = 5.5(\frac{a}{h_w})^{0.8}\tan(\Phi) + 8.7\left(\frac{a}{h_w}\right)^{-0.8} \tag{3}$$

An additional validation is conducted as follows considering a simply supported plate, with dimensions $a/h_0 = 2$, and $h_1/t_w = 200$. Table 3 presents a comparison between the shear buckling coefficients computed through the finite element model and the those obtained with Eqs. (2) and (3). It is worth pointing out that the value used for h in Eq. (2) is the major height $h=h_1$.

<p align="center">Table 3: Model validation</p>

Φ	k_s FEM	k_s Eq.(2)	k_s Eq. (3)	k_s^{FEM} / k_s Eq.(2)	k_s FEM / $k_s^{Eq. (3)}$
0	6.67	6.34	6.59	1.05	1.01
5	8.08	7.17	8.77	1.13	0.92
10	8.78	7.70	9.65	1.14	0.91
20	9.48	8.33	10.46	1.14	0.91
30	10.97	9.98	11.95	1.10	0.92

According to the presented results, with differences between the model and the literature of less than 15%, the model is then validated.

3. Parametric study

For the sake of generalization, the effect of five variables in the shear buckling coefficient is studied. The variables are: The flexural rigidity of the stiffener γ_s, the web slenderness h_1/t_w, the ratio of flange thickness to web thickness t_f /t_w, the aspect ratio a/h_0 and the haunch inclination $tan(\Phi)$. The different values of the parameters are shown in Table 1, resulting in 2025 cases to run. The analysis of the results is presented next.

3.1 Influence of the stiffener position and flexural rigidity γ_s

The stiffener flexural rigidity is defined as:

$$\gamma_s = 10.9\frac{I_{st}}{h_w t_w{}^3} \tag{4}$$

where I_{st} is the second moment of area of the stiffener respect to an axis placed at the centroid of the area including the stiffener and a portion of the web of $15t_w$ on each side as defined by the Eurocode (EC3, 2006). This code also states that when calculating the shear buckling coefficient, the value of the second moment of area must be divided by three.

Fig. 5 shows the variation of the buckling coefficient k_s in terms of γ_s. The main analysis is that after a reaching a certain value of γ_s, there is not a significant increase of the value of k_s. This value is the transition between the behavior of a weak stiffener and the behavior of a strong stiffener. As presented in the previous plots, the value of minimum rigidity for a strong stiffener is $\gamma_s=20$. After this value the buckling coefficient remain almost constant, therefore the conclusion is that for a strong stiffener, there is no influence of the flexural rigidity on the value of k_s. Subsequently, the following analyses are performed using only strong stiffeners.

(a) $\phi = 10°$ (b) $\phi = 15°$

(c) $\phi = 20°$ (d) $\phi = 30°$
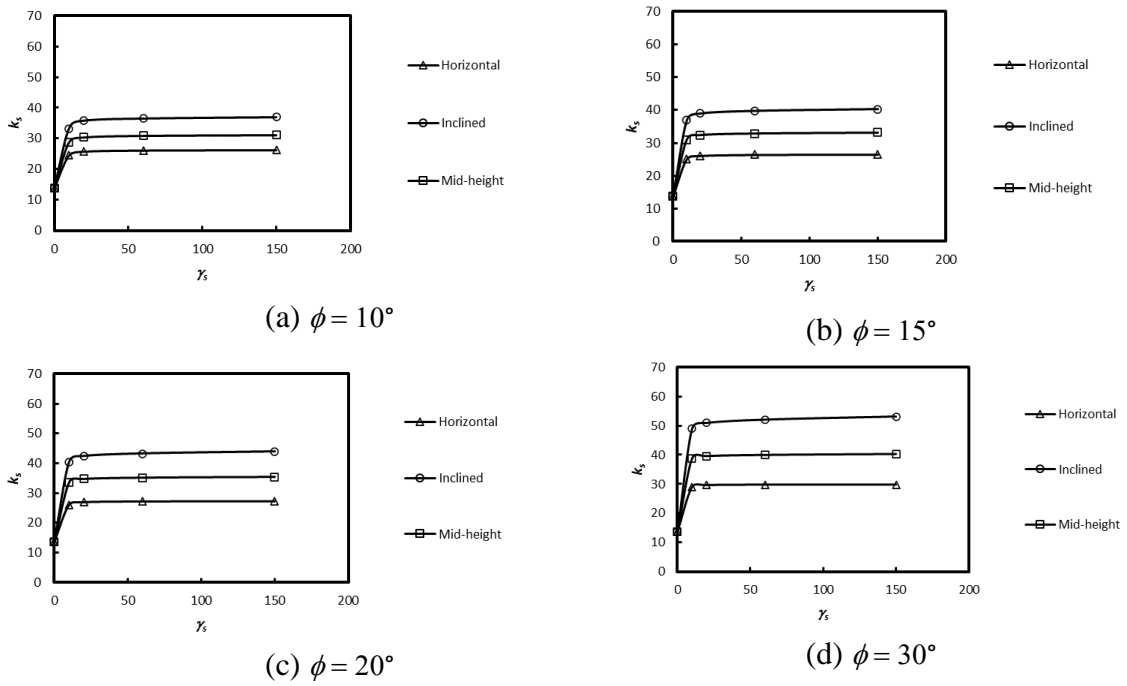
Figure 5: Buckling coefficients k_s in terms of γ_s $(a/h_o=1, h_1/t_w =300, t_f/t_w=1)$.

(a) Horizontal stiffener   (b) Inclined stiffener

(c) Mid-height stiffener
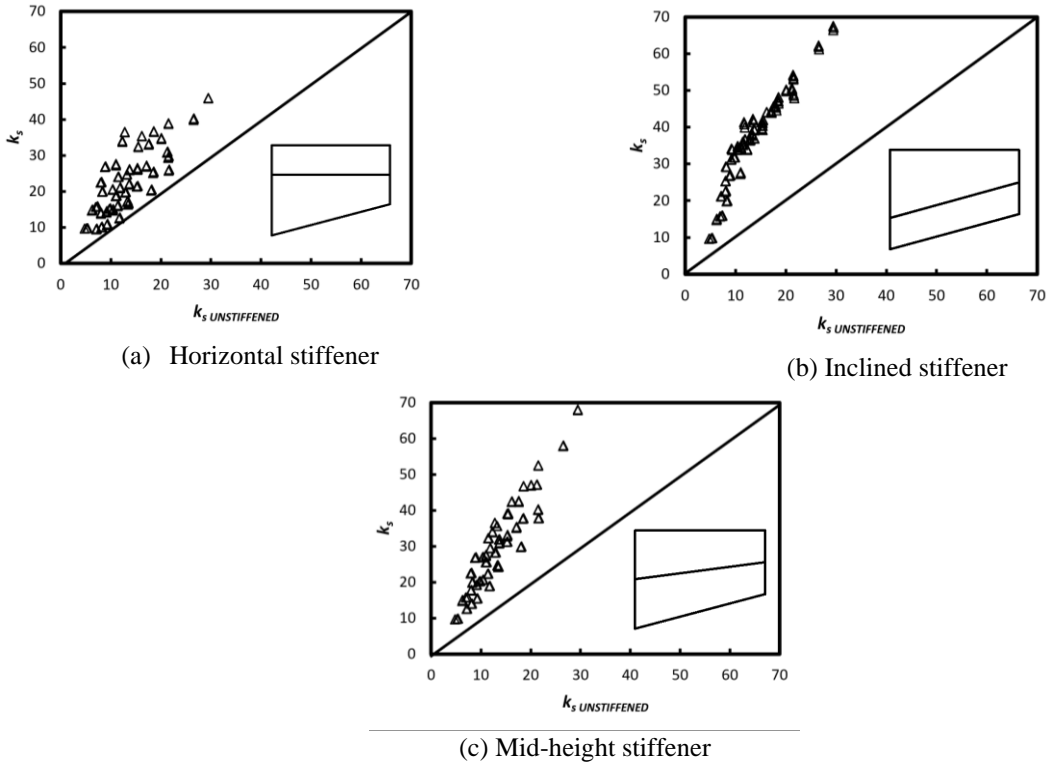
Figure 6: Influence of the stiffener placement.

Fig. 6 shows a significant enhancement in the buckling coefficient with the usage of a longitudinal stiffener. On average, the use of a strong horizontal stiffener increases k_s by a 78% (Fig. 6a). A strong stiffener placed parallel to the inclined flange increases k_s on the average by a 179% (Fig. 6b), and a strong stiffener placed at both of mid heights increases k_s by a 124% (Fig. 6c).

3.2 Influence of the web slenderness h_1/t_w

Fig. 7 shows the variation of k_s with respect to the web slenderness h_1/t_w, for $\gamma_s = 150$, $a/h_0 = 2$ and $t_f/t_w = 2$.

(a) $\phi = 10°$ (b) $\phi = 15°$

(c) $\phi = 20°$ (d) $\phi = 30°$
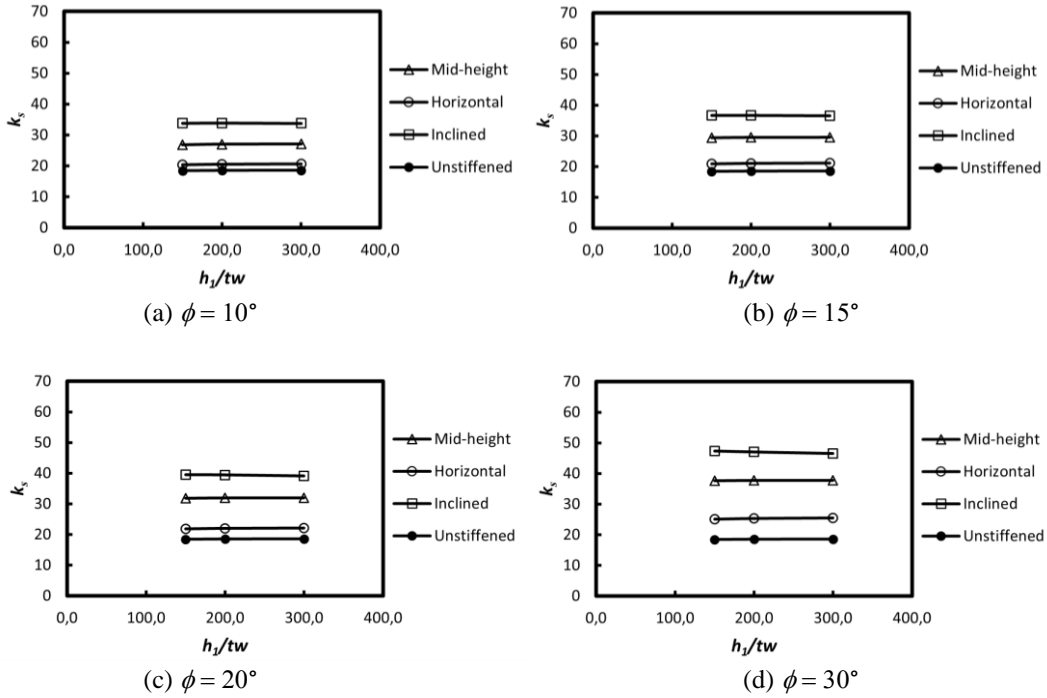
Figure 7: Buckling coefficients k_s in terms of h_1/t_w ($\gamma_s = 150$, $a/h_0 = 2$, $t_f/t_w = 2$)

It is clearly observed that the slenderness parameter h_1/t_w has a diminished impact on the shear buckling coefficient, as long as the web is slender $h_1/t_w > 150$ and the code limit is maintained $h_1/t_w < 300$ (AASHTO 2020). For this reason, the following results will not include the aforementioned parameter.

3.3 Influence of the thickness ratio t_f/t_w

From Fig. 8 to Fig. 11 the variation of buckling coefficient k_s in terms of t_f/t_w is shown.

(a) $a/h_0 = 1$ (b) $a/h_0 = 2$ (c) $a/h_0 = 3$
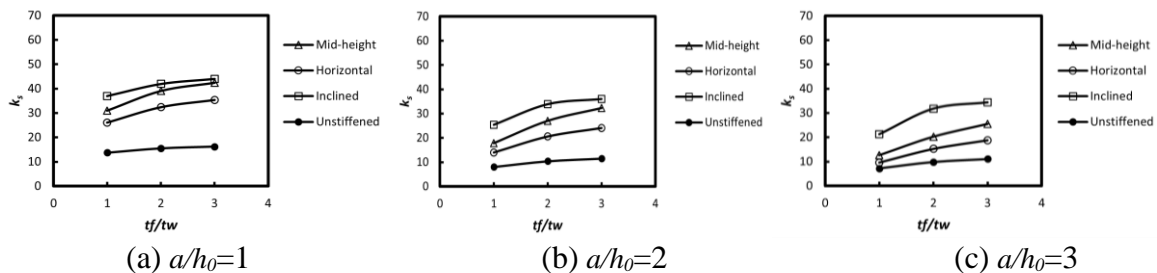
Figure 8: Buckling coefficients k_s in terms of t_f/t_w ($\gamma_s = 150$, $\phi = 10°$)

(a) $a/h_o=1$ (b) $a/h_o=2$ (c) $a/h_o=3$
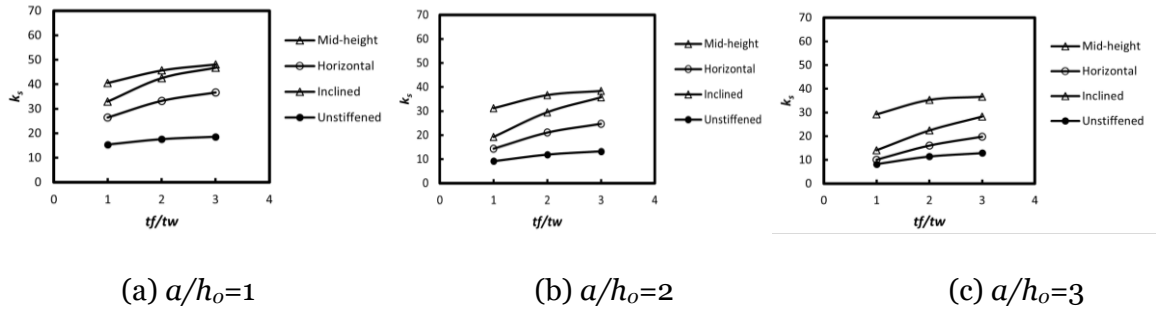
Figure 9: Buckling coefficients k_s in terms of t_f/t_w (γ_s =150, ϕ = 15°)

(a) $a/h_0=1$ (b) $a/h_0=2$ (c) $a/h_0=3$
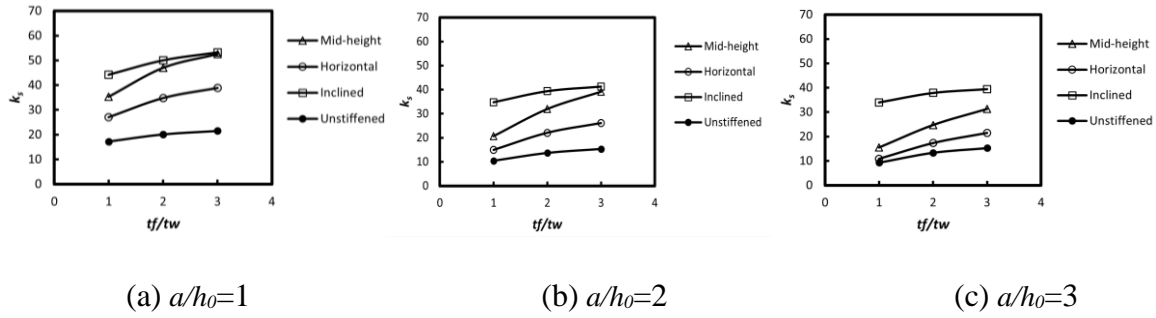
Figure 10: Buckling coefficients k_s in terms of t_f/t_w (γ_s =150, ϕ = 20°)

(a) $a/h_0=1$ (b) $a/h_0=2$ (c) $a/h_0=3$
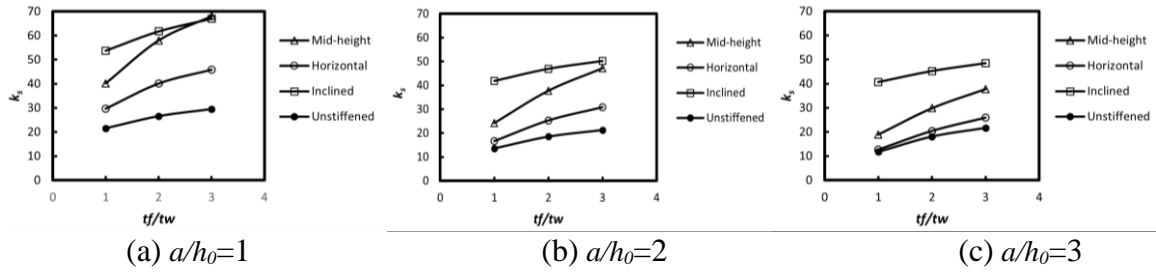
Figure 11: Buckling coefficients k_s in terms of t_f/t_w (γ_s =150, ϕ = 30°)

It is observed that for all cases, there is an increase in the buckling coefficient as the flange-to-web thickness ratio is greater. This is expected, as the thickness of the flanges increase, the boundary condition of the web to flange juncture approaches to a fixed support, thus increasing the rigidity and the shear capacity of the girder. As the variation of this ratio makes the buckling coefficient change, this value is included in the analysis.

3.4 Influence of the panel aspect ratio a/h_0

From Fig. 12 to Fig. 15, the variation of the buckling coefficient k_s in terms of the aspect ratio a/h_0 is presented.
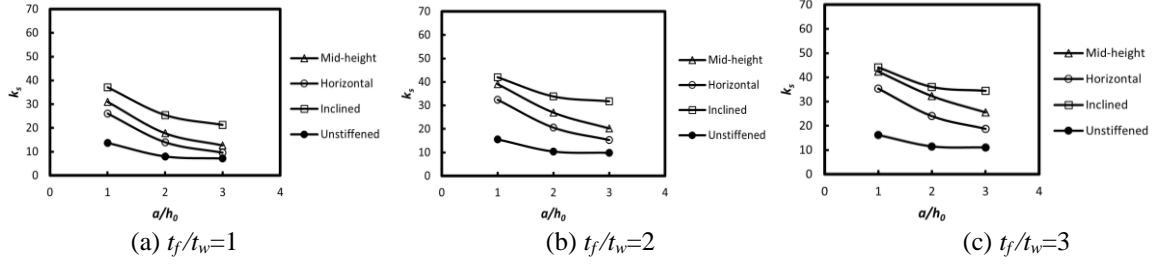
Figure 12: Buckling coefficients k_s in terms of a/h_o (γ_s =150, $\phi = 10°$)

(a) $t_f/t_w=1$ (b) $t_f/t_w=2$ (c) $t_f/t_w=3$

(a) $t_f/t_w=1$ (b) $t_f/t_w=2$ (c) $t_f/t_w=3$
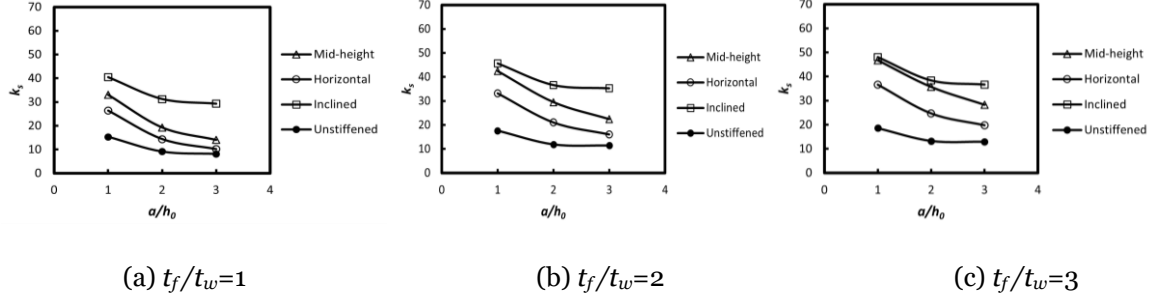
Figure 13: Buckling coefficients k_s in terms of a/h_o (γ_s =150, $\phi = 15°$)

(a) $t_f/t_w=1$ (b) $t_f/t_w=2$ (c) $t_f/t_w=3$
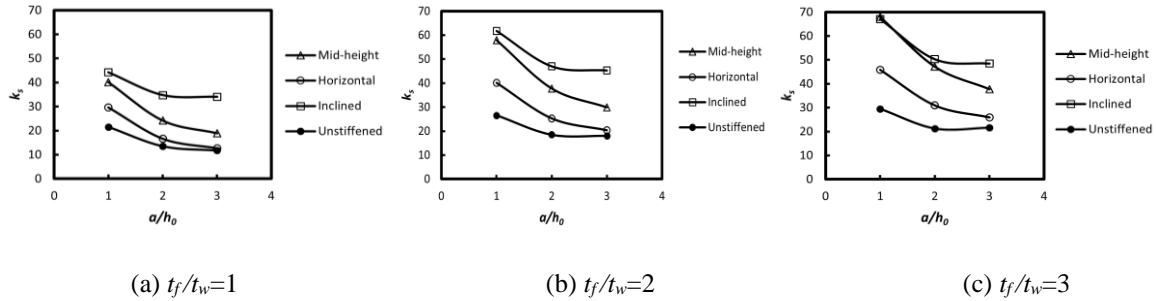
Figure 14: Buckling coefficients k_s in terms of a/h_o (γ_s =150, $\phi = 20°$)

(a) $t_f/t_w=1$ (b) $t_f/t_w=2$ (c) $t_f/t_w=3$
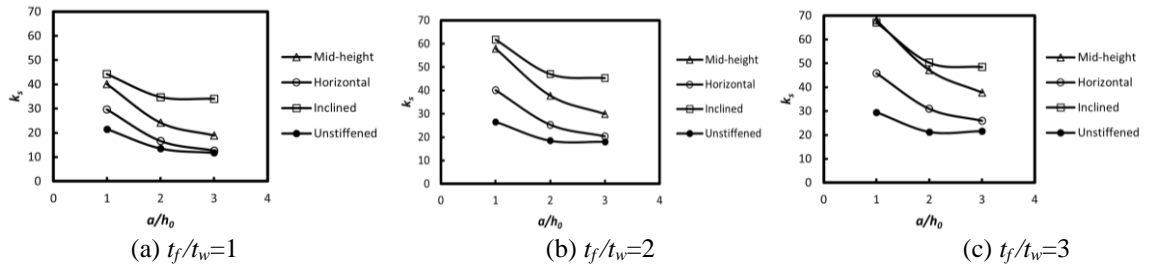
Figure 15: Buckling coefficients k_s in terms of a/h_o (γ_s =150, $\phi = 30°$)

It is observed that for all cases, as the aspect ratio increases, the buckling coefficient decreases. This is explained because as the panel aspect ratio increases, the panel is longer and bending stresses increase, thus reducing shear buckling capacity. As this parameter makes the buckling coefficient change, this value must be included in the analysis.

3.5 Influence of the haunch inclination tan(ϕ)
From Fig. 16 to Fig. 18 the variation of the buckling coefficient in terms of the haunch inclination $tan(\phi)$ is presented.

84

(a) $a/h_0=1$ (b) $a/h_0=2$ (c) $a/h_0=3$
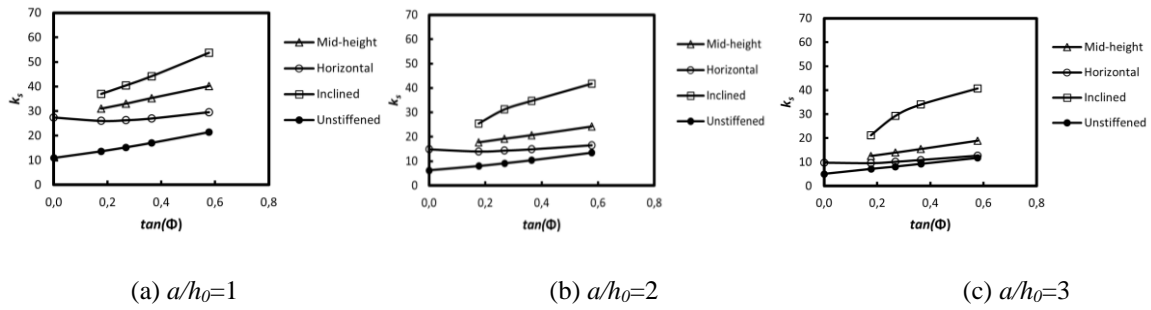
Figure 16: Buckling coefficients k_s in terms of $tan(\phi)$ (γ_s =150, t_f/t_w=1)

(a) $a/h_0=1$ (b) $a/h_0=2$ (c) $a/h_0=3$
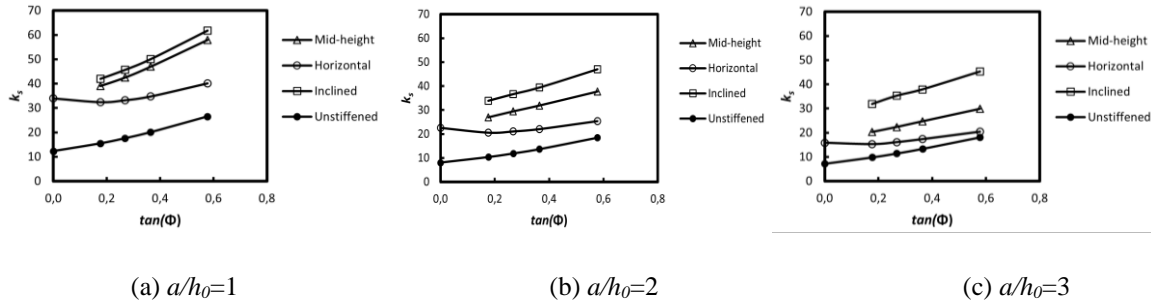
Figure 17: Buckling coefficients k_s in terms of $tan(\phi)$ (γ_s =150, t_f/t_w=2)

(a) $a/h_0=1$ (b) $a/h_0=2$ (c) $a/h_0=3$
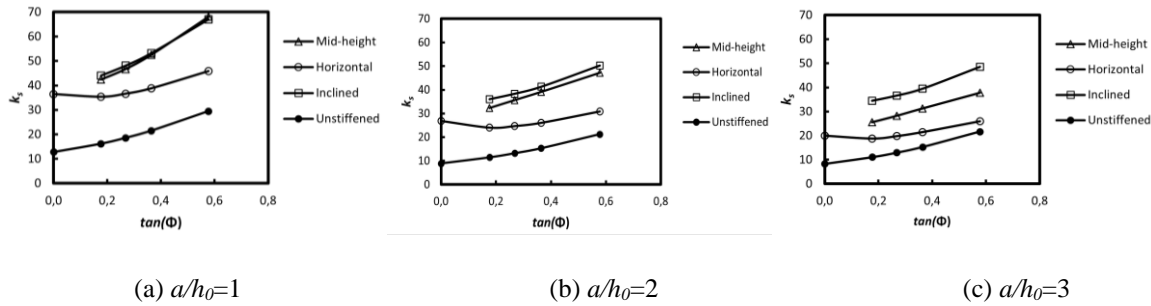
Figure 18: Buckling coefficients k_s in terms of $tan(\phi)$ (γ_s =150, t_f/t_w=3)

It is observed that for all cases, as the haunch angle ϕ increases the buckling coefficient also increases. As this parameter affects the buckling coefficient, this value must be included in the analysis.

3.5 Buckling shapes.

Fig. 19 shows the buckling shapes, varying the stiffener rigidity and position, for a girder

with $a/h_0=2$, t_f/t_w=2, h_1/t_w = 200, ϕ = 20°. Observing the deformed shapes in Fig. 19, the

following findings are highlighted:

1. When the panel is unstiffened γ_s= 0, the buckling shape involves the whole web panel, thus reducing the capacity (k_s = 13.70).
2. When the stiffener is weak γ_s = 10, the stiffener does not provide a nodal line of near zero out-of-plane displacement, and the buckling also involves the whole web panel and the stiffener. Nevertheless, the buckling coefficient k_s increases compared to the unstiffened girder.

3. When the stiffener is strong, γ_s = 20, buckling occurs only in the larger sub-panel, as the stiffener restricts the out-of-plane displacement similar to a nodal line with near zero displacements, thus dividing the whole web panel into two sub-panels, and increasing the capacity of the girder to resisting shear buckling. For γ_s = 150 the difference in the buckling coefficient is very small compared to that obtained for a stiffener with γ_s = 20
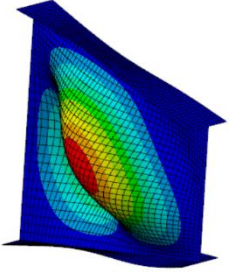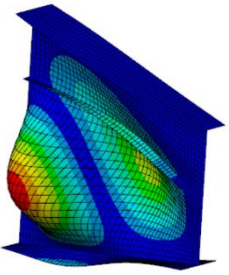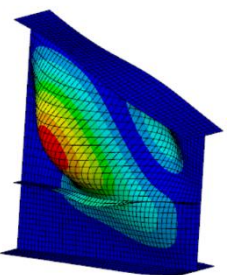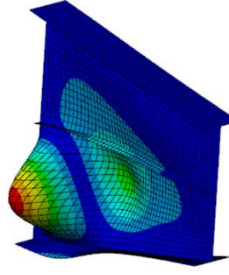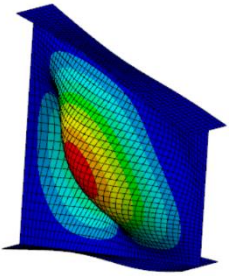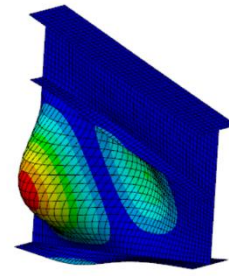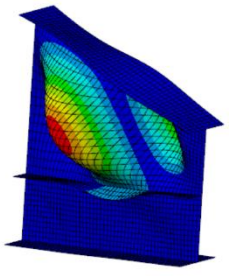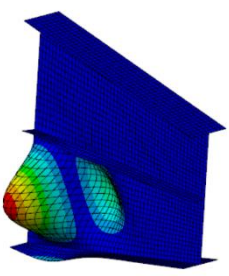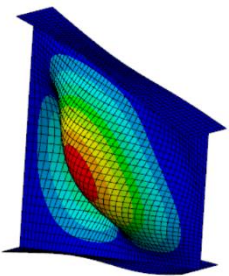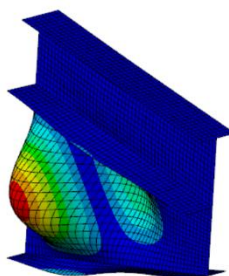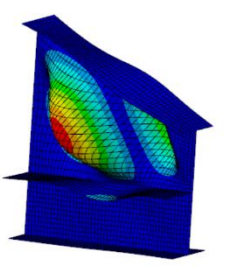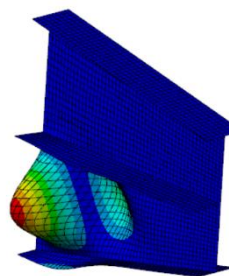
γ_s	Stiffener position			
	Unstiffened	Horizontal	Inclined	Mid-Height
10	k_s = 13.70	k_s = 20.21	k_s = 33.23	k_s = 30.44
20	k_s = 13.70	k_s = 21.65	k_s = 37.45	k_s = 31.45
150	k_s = 13.70	k_s = 22.06	k_s = 39.44	k_s = 31.96

Figure 19: Buckling shapes for a/h_o=2, t_f/t_w=2, h_1/t_w = 200, $\phi = 20°$.

4. Proposal of buckling coefficient

4.1 Procedure

The following procedure was used to develop the prediction models for each of the stiffener positions: horizontal, inclined and Mid-Height.

1. Determine the variables that may influence in the estimation of the buckling coefficient. The selected variables were: t_f/t_w, a/h_0 and $tan(\phi)$. It was found that the influence of the web slenderness ratio, h_1/t_w, can be neglected.
2. It was established that all the equations were going to be set for strong stiffeners.

3. Construct the dependence charts, for all the possible combinations of angles and t_f /t_w, it revealed the relationships between the aspect ratio a/h_0 and the buckling coefficient.
4. Once the trendlines of the charts were established, in the form $y(x)=C_o(x)^\alpha$, where $y(x)$ corresponds to the buckling coefficient and (x) to the aspect ratio, the coefficients were tabulated (C_o vs α).
5. The relationship between C_o and α with the parameter $tan(\phi)$ were found plotting them again as shown from Fig. 20 to Fig. 22.

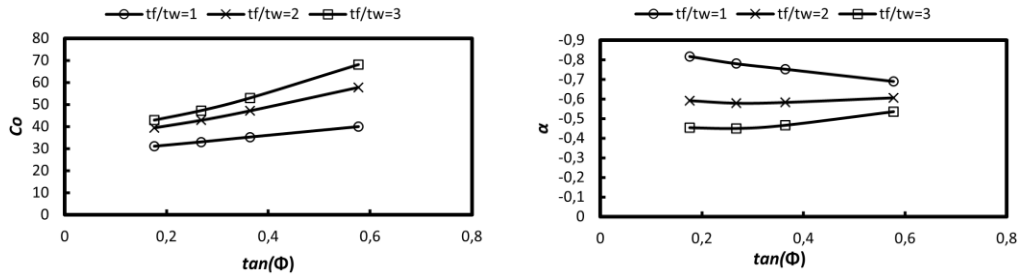

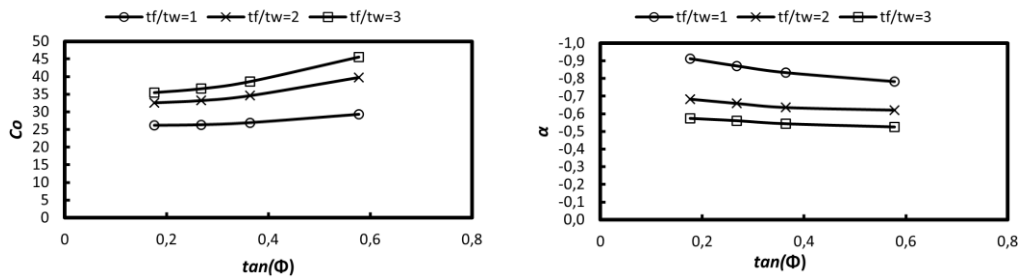Figure 20: C_o and α in terms of $tan(\phi)$ for Mid-Height position.

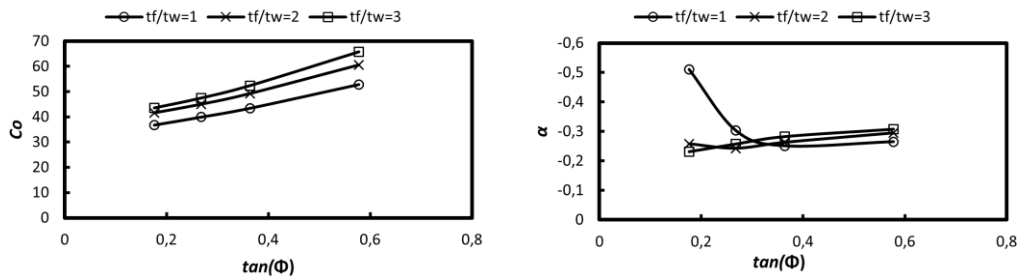Figure 21: C_o and α in terms of $tan(\phi)$ for horizontal position.

Figure 22: C_o and α in terms of $tan(\phi)$ for inclined position.

6. Polynomial trendlines were made again to fit the formulas that describe C_o and α.
7. A new set of variables a and b were plotted in terms of thickness ratio t_f/t_w, in order to involve all the parameters affecting the buckling coefficient. The plots are shown from Fig. 23 to Fig. 25.
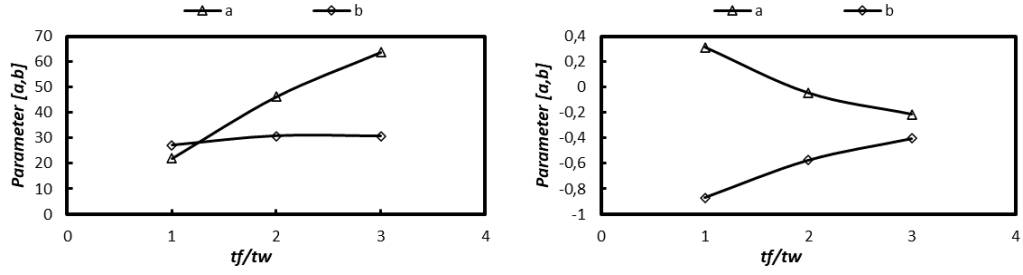
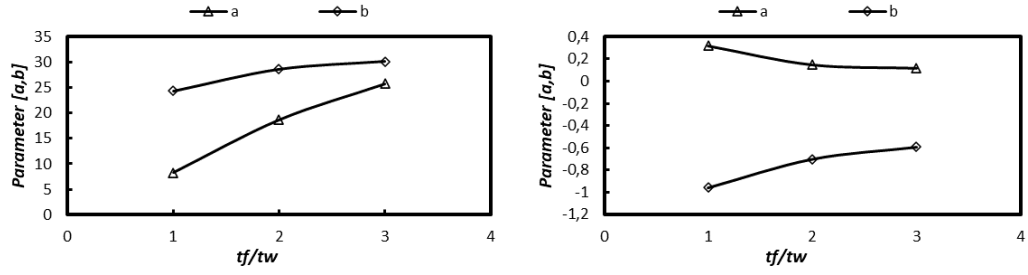Figure 23: a and b in terms of t_f/t_w for mid-height position.

Figure 24: a and b in terms of t_f/t_w for horizontal position.
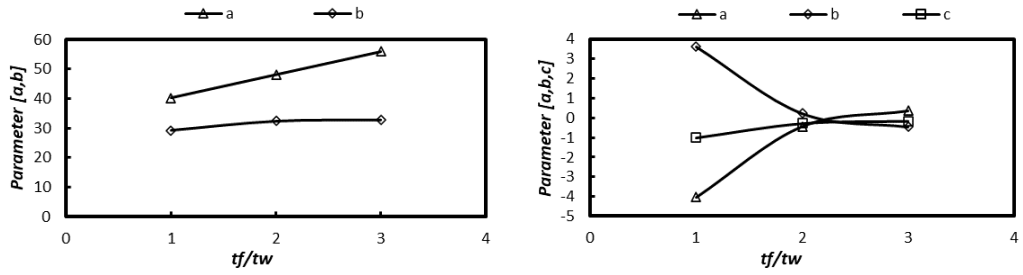

Figure 25: a and b in terms of t_f/t_w for inclined position.

8. In a hierarchical way, the equation proposed in 3) was rewritten with steps 4) and 5), in order to obtain the final equations.

Mid-Height:

$$k_s = \left[\left(20.8 \cdot \frac{t_f}{t_w} + 2.4\right) \cdot tan\theta + 1.8 \cdot \frac{t_f}{t_w} + 26\right] \cdot \left(\frac{a}{h_0}\right)^{\left[\left(-0.2\frac{t_f}{t_w}+0.5\right)\cdot tan\theta + 0.2\cdot\frac{t_f}{t_w}-1.1\right]} \tag{5}$$

Horizontal:

$$k_s = 0.95 \cdot \left[\left(8.7 \cdot \frac{t_f}{t_w} + 0.1\right) \cdot tan\theta + 2.9 \cdot \frac{t_f}{t_w} + 22\right] \left(\frac{a}{h_0}\right)^{\left[\left(-0.1\frac{t_f}{t_w}+0.4\right)\cdot tan\theta + 0.2\cdot\frac{t_f}{t_w}-1.1\right]} \tag{6}$$

Inclined:

$$k_s = \left[\left(7.9 \cdot \frac{t_f}{t_w} + 32.4\right) \cdot tan\theta + 1.8 \cdot \frac{t_f}{t_w} + 28\right] \cdot \left(\frac{a}{h_0}\right)^{(-0.29)} \tag{7}$$

4.2 Statistical evaluation

Fig. 26 shows the correlation between the computed buckling coefficient and those obtained with Eqs. (5), (6) and (7). It can be seen that the best correlation is attained for the girder stiffened at mid-height with $R^2=0.99$, for the stiffener placed horizontally $R^2=0.95$, and finally for the stiffener placed parallel to the inclined flange $R^2=0.91$.

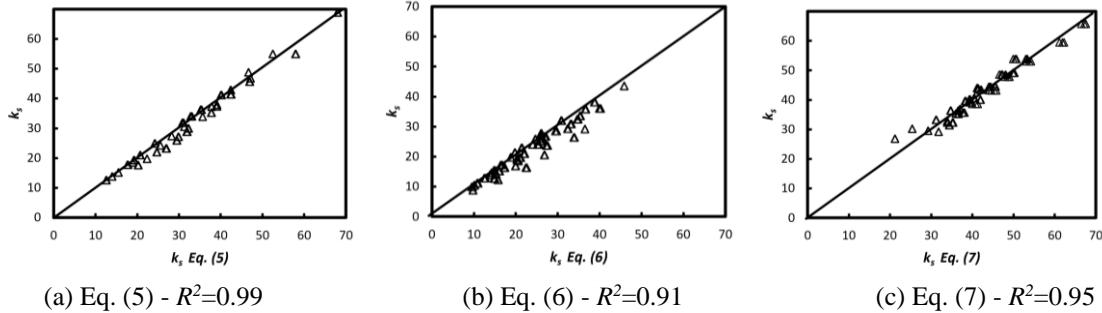(a) Eq. (5) - $R^2=0.99$ (b) Eq. (6) - $R^2=0.91$ (c) Eq. (7) - $R^2=0.95$

Figure 26. Correlation between numerical results and proposed formulas

5. Conclusions

In this paper, the critical buckling response of longitudinally stiffened-haunched steel plate girders subjected to shear loading was investigated through finite elements analysis. An extensive parametric study was performed varying the panel aspect ratio, the flange-to-thickness ratio, the stiffener rigidity and location (mid height, horizontal and inclined). From the results the following conclusion are drawn:

.- The use of longitudinal stiffeners increases the critical buckling coefficient k_s, and hence the critical stresses, of haunched girders subjected to shear loading.

.- Among the investigated parameters, the slenderness of the panel h_1/t_w has a negligible impact on the buckling coefficients.

.- Regarding the flexural rigidity of the stiffener, within the range of parameters evaluated herein there is a diminished influence for $\gamma_s \geq 20$. Beyond this limit, buckling of the webpanel is divided into two subpanels, and the whole girder attains a greater buckling load. The highest buckling coefficients were attained when the longitudinal stiffener was located parallel to the inclined flange.

.-Locating the stiffener parallel to the inclined flange works the best.

.- Buckling coefficients calculated with the proposed formulas attained very high correlation with the values computed numerically.

References

AASHTO (2020). AASHTO LRFD Bridge Design Specifications. 9th Edition, American Association of State Highway and Transportation Officials, Washington, DC.

ANSYS. Ansys Release 2022 R1

AbdelAleem, B.H., Ismail, M.K., Haggag, M., El-Dakhakhni, W., Hassan, A.A. (2022). "Interpretable soft computing predictions of elastic shear buckling in tapered steel plate girders." *Thin-Walled Structures*, 176, 109313.

Bedynek, A., Real, E., Mirambell, E. (2013). "Tapered plate girders under shear: Tests and numerical research." *Engineering Structures*, 46, 350-358.

Bedynek, A.E., Mirambell, E. (2013). "Shear buckling coefficient for simply-supported tapered plates subjected to shear." *Proceedings of the Institution of Civil Engineers – Structures and Buildings*; 166.

Bedynek, A., Mirambell, E., Real, E. (2013). "Experimental and numerical research on longitudinally stiffened tapered steel plate girders subjected to shear." *In Research and Applications in Structural Engineering, Mechanics and Computation* (pp. 459-460). CRC Press.

Bedynek, A. "Structural behavior of tapered steel plate girders subjected to shear." Doctoral Dissertation, Construction Engineering Department, Universitat Politécnica de Catalunya, 2014. Available at: <http://hdl.handle.net/2117/95340>.

Bedynek, A., Real, E., Mirambell, E. (2014) "Shear buckling coefficient: proposal for tapered steel plates." *Proceedings of the Institution of Civil Engineers - Structures and Buildings* 167(4): 243-252.

Bedynek, A., Real, E., Mirambell, E. (2017). "Design proposal for ultimate shear strength of tapered steel plate girders." *Informes de la Construcción*, 69(545), 1-12.

Eurocode 1993-1-5: Eurocode 3 (EC3): Design of Steel Structures – Part 1-5. 2006.

Hassanein, M.F., Kharoob, O.F. (2014). "Shear buckling behavior of tapered bridge girders with steel corrugated webs." *Engineering Structures*, 74, 157-169.

Hassanein, M.F., Kharoob, O.F. (2015). "Linearly tapered bridge girder panels with steel corrugated webs near intermediate supports of continuous bridges." *Thin-Walled Structures*, 88, 119-128.

Ibrahim, M.M., El-Aghoury, I.M., Ibrahim, S.A.B. (2020). "Finite element investigation on plate buckling coefficients of tapered steel members web plates." *Structures*, 28, 2321-2334).

Ibrahim, M.M., El Aghoury, I.M., Ibrahim, S.A.B. (2020). "Experimental and numerical investigation of ultimate shear strength of unstiffened slender web-tapered steel members." *Thin-Walled Structures*, 148, 106601.

Kuhlmann, U., Breunig, S., Gölz, L.M., Pourostad, V., Stempniewski, L. (2020). "New developments in steel and composite bridges." *Journal of Constructional Steel Research*, 174, 106277.

Mirambell, E., Zárate, V. (2000). "Web buckling of tapered plate girders." *Proceedings of the Institution of Civil Engineers - Structures and Buildings*, 140(1), 51-60.

Pourostad, V., Kuhlmann, U. (2018). "Experimental investigations on girders with non-rectangular panels". *Eighth International Conference on Thin-Walled Structures - ICTWS 2018*, Lisbon, Portugal.

Pourostad, V., Kuhlmann, U. (2019). "Experimental and numerical investigations of unstiffened steel girders with non-rectangular panels subjected to bending and shear." *The International Colloquium on Stability and Ductility of Steel Structures - SDSS 2019*, Prague, Czech.

Pourostad, V., Kuhlmann, U. (2021). "New development of design rules for girder with non-rectangular slender web." *ce/papers*, 4(2-4), 1797-1804.

Real, E., Bedynek, A., Mirambell, E. (2010). "Numerical and experimental research in tapered steel plate girders subjected to shear." *Proceedings of SDSS'Rio 2010: International Colloquium Stability and Ductility of Steel Structures*, Rio de Janeiro, Brazil, 747-754.

Sediek, O.A., Safar, S.S., Hassan, M.M. (2020). "Numerical investigation on shear strength of tapered perfect end web panels." *Structures*, 28, 354-368.

Timoshenko S.P., Gere J.M. (1936). Theory of elastic stability. Courier Corporation.

Zárate AV, Mirambell, E. (2004). "Shear strength of tapered steel plate girders." *Proceedings of the Institution of Civil Engineers – Structures and Buildings*, 157(5), 343-54.

Zevallos, E., Hassanein, M.F., Real, E., Mirambell, E. (2016). "Shear evaluation of tapered bridge girder panels with steel corrugated webs near the supports of continuous bridges." *Engineering Structures*, 113, 149-159.

Ziemian, R. D. (Ed.). (2010). Guide to stability design criteria for metal structures. John Wiley & Sons.